t-channel dilepton production and anisotropy in pion nucleon collisions

Dileptonerzeugung und -anisotropie in Pion Nucleon Kollisionen im t-Kanal
Master-Thesis von Deniz Aydın Nitt aus Nordhorn
Tag der Einreichung:

1. Gutachten: PD Dr. Michael Buballa
2. Gutachten: Prof. Dr. Tetyana Galatyuk

TECHNISCHE UNIVERSITÄT DARMSTADT

Institut für Kernphysik
Theoriezentrum
Nuclei, Hadrons & Quarks

t-channel dilepton production and anisotropy in pion nucleon collisions
Dileptonerzeugung und -anisotropie in Pion Nucleon Kollisionen im t-Kanal

Vorgelegte Master-Thesis von Deniz Aydın Nitt aus Nordhorn

1. Gutachten: PD Dr. Michael Buballa
2. Gutachten: Prof. Dr. Tetyana Galatyuk

Tag der Einreichung:

Bitte zitieren Sie dieses Dokument als:
URN: urn:nbn:de:tuda-tuprints-123
URL: http://tuprints.ulb.tu-darmstadt.de/123

Dieses Dokument wird bereitgestellt von tuprints,
E-Publishing-Service der TU Darmstadt
http://tuprints.ulb.tu-darmstadt.de
tuprints@ulb.tu-darmstadt.de

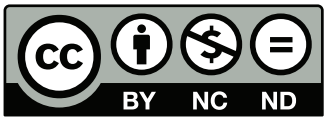

Die Veröffentlichung steht unter folgender Creative Commons Lizenz:
Namensnennung – Keine kommerzielle Nutzung – Keine Bearbeitung 2.0 Deutschland
http://creativecommons.org/licenses/by-nc-nd/2.0/de/

Erklärung zur Abschlussarbeit gemäß § 22 Abs. 7 und § 23 Abs. 7 APB TU Darmstadt

Hiermit versichere ich, Deniz Aydın Nitt, die vorliegende Master-Thesis / Bachelor-Thesis gemäß § 22 Abs. 7 APB der TU Darmstadt ohne Hilfe Dritter und nur mit den angegebenen Quellen und Hilfsmitteln angefertigt zu haben. Alle Stellen, die Quellen entnommen wurden, sind als solche kenntlich gemacht worden. Diese Arbeit hat in gleicher oder ähnlicher Form noch keiner Prüfungsbehörde vorgelegen. Mir ist bekannt, dass im Falle eines Plagiats (§38 Abs.2 APB) ein Täuschungsversuch vorliegt, der dazu führt, dass die Arbeit mit 5,0 bewertet und damit ein Prüfungsversuch verbraucht wird. Abschlussarbeiten dürfen nur einmal wiederholt werden. Bei der abgegebenen Thesis stimmen die schriftliche und die zur Archivierung eingereichte elektronische Fassung gemäß § 23 Abs. 7 APB überein. Bei einer Thesis des Fachbereichs Architektur entspricht die eingereichte elektronische Fassung dem vorgestellten Modell und den vorgelegten Plänen.

English translation for information purposes only:

Thesis Statement pursuant to § 22 paragraph 7 and § 23 paragraph 7 of APB TU Darmstadt I herewith formally declare that I, Deniz Aydın Nitt, have written the submitted thesis independently pursuant to § 22 paragraph 7 of APB TU Darmstadt. I did not use any outside support except for the quoted literature and other sources mentioned in the paper. I clearly marked and separately listed all of the literature and all of the other sources which I employed when producing this academic work, either literally or in content. This thesis has not been handed in or published before in the same or similar form. I am aware, that in case of an attempt at deception based on plagiarism (§38 Abs. 2 APB), the thesis would be graded with 5,0 and counted as one failed examination attempt. The thesis may only be repeated once. In the submitted thesis the written copies and the electronic version for archiving are pursuant to § 23 paragraph 7 of APB identical in content. For a thesis of the Department of Architecture, the submitted electronic version corresponds to the presented model and the submitted architectural plans.

Datum / Date: Unterschrift/Signature:

Abstract

The goal of this thesis is to investigate the dilepton anisotropy of the interaction $\pi N \to \pi e^- e^+$ with focus on the impact of the t-channel. This work builds upon the results of Speranza, Zétényi, and Friman [1] [2] who have already studied dilepton anisotropy for the abovementioned process in the resonant s- and u-channels. We follow their approach and employ effective Lagrangians to extend their results for the dominant nucleon resonances for intermediate π, ρ-meson and a_1. We study the process for a CM energy of $\sqrt{s} = 1.49\,\text{GeV}$ and various dilepton masses, ranging from 100 MeV to 500 MeV.

Zusammenfassung

Das Ziel dieser Masterarbeit ist es die Dileptonenanisotropie in der Teilcheninteraktion $\pi N \rightarrow \pi e^- e^+$ zu untersuchen. Dabei liegt das Hauptaugenmerk auf dem Einfluss des t-Kanals. Diese Arbeit baut auf den Ergebnissen von Speranza, Zétényi und Friman [1] [2] auf, die bereits Dileptonenanisotropie für den oben genannten Prozess in den Resonanten s- und u-Kanälen untersucht haben. Wir folgen ihrer Herangehensweise und benutzen effektive Lagrange-Dichten, um ihre Ergebnisse für die dominanten Nukleonresonanzen zu erweitern. Dabei betrachten wir virtuelle π, ρ-Mesonen und die a_1-Resonanz im T-Kanal. Wir halten die Schwerpunktsenergie bei $\sqrt{s} = 1.49\,\text{GeV}$ und betrachten verschiedene Dileptonenmassen von 100 MeV to 500 MeV.

Contents

1 Introduction

The theory of nuclear and particle physics helps us in understanding how our world and the universe work. In order to find new information and test existing theories, one can study spin dependencies of hadronic interactions, which allow us to deduce the underlying mechanisms. Hadronic interactions are typically found in heavy ion collisions. However it is difficult to study the strongly interacting matter directly because there are secondary reactions in the collision volume. Therefor electromagnetic probes such as photons and dileptons can be used [3] since they do not interact strongly and hence their mean free path is expected to be larger than the transverse size of the collision volume. A dilepton pair can be created by the decay of a virtual photon, which according to quantum field theory is a photon with non vanishing rest mass that can briefly exist before decaying into an electron positron pair under the rules of quantum electrodynamics. The leptons then carry on the polarisation information of the decayed photon. This can be revealed by studying the angular distribution of the dilepton pair, which is for example done in the High Acceptance Di-Electron Spectrometer HADES [4]. Not only photons can be virtual. Particles in a collision can join an intermediate state, which in case of πN-collision can be a nucleon resonance or a Δ-baryon. The incoming particle can also interact by exchanging an intermediate particle. All virtual particles have in common that they, as opposed to their real counterparts, can not be observed. However, of course they still contribute to the overall process and as such their share is also reflected in the photon and dilepton polarisation. This allows us to get valuable insight in the role of different particles and the overall interaction of hadronic matter.

A lot of work has been dedicated to investigate the emergence of dilepton pairs such as [4] [5] [6]. For the interpretation of the results, a good understanding of the reactions is required. Speranza, Zétényi, and Friman [1] [2] investigated the angular anisotropy of $\pi N \rightarrow Ne^+e^-$theoretically with focus on the s- and u-channel of the interaction. This allows to draw conclusions about the intermediate nucleon resonances, that only contribute in these two channels. By implementing various resonances around the HADEScenter of mass energy $\sqrt{s} = 1.49\,\text{GeV}$ they were able to identify the two dominant resonances N(1440) and N(1535). To study the anisotropy they came up with the novel concept of anisotropy coefficients which reflect the polarisation state of the virtual photon [2]. Despite the first successes of this model, it is still incomplete because it lacks the t-channel contributions. It is the goal of this thesis to give a more complete picture. We follow the approach of Speranza and aim to calculate the anisotropy coefficients including the t-channel with intermediate π, ρ-mesons and a_1-resonances in the overall process.

2 The process $\pi N \to Ne^+e^-$

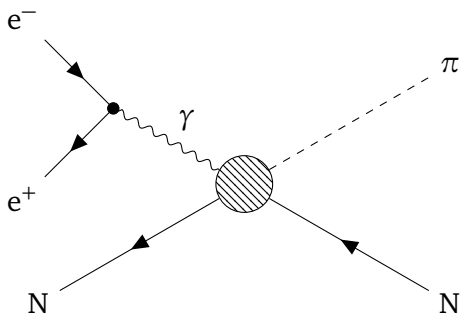

Figure 2.1.: The process $N\pi \to Ne^+e^-$. Here and in all other Feynman diagrams the direction of time is right to left.

In this thesis we investigate the interaction $N\pi \to Ne^+e^-$, as depicted in Figure 2.1. This chapter is ultimately designed to derive the anisotropy coefficients. However we first have to take a closer look at the underlying processes. We will follow the idea of Speranza [2] and treat the process as a special case of a more general version, where we have an initial state that produces a spin-1 particle V and another particle P. The spin-1 particle then decays into two fermions F_1 and F_2, so we have the total process

$$\text{initial state} \to V + P \to P + F_1 + F_2. \tag{2.1}$$

If we make the assumption, that V and P do not interact with one another once produced, we can split the process into two parts, namely the production mechanism which produces V and P and is described by the matrix element $\mathcal{M}^{\text{prod}}(\lambda)$; and the decay mechanism following described by $\mathcal{M}^{\text{decay}}(\lambda)$. Thus, this chapter is constructed as follows: We start with briefly revisiting quantum field theory in order to derive the decay matrix element for which we also discuss the polarisation vectors of spin-1 particles. Afterwards we will introduce the anisotropy coefficients which are the central element of this thesis. To calculate them we will then discuss Rarita-Schwinger fields, isospin, the vector meson dominance model and the interactions between all concerned particles in order to finally compute the production matrix element.

2.1 Relativistic QFT I: Klein-Gordon-, Dirac- and Proca-Field

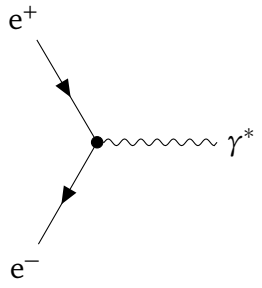

Figure 2.2.: The decay process $\gamma^* \to e^-e^+$, for a $e^\pm$ with corresponding four momentum $p^\pm$ and spin $s^\pm$.

In our case, we have the decay $\gamma^* \to e^+e^-$, as shown in Figure 2.2. In order to write down the matrix element, we will briefly revisit the underlying relativistic quantum field theories, based on Peskin and Schroeder [7] and Greiner and Reinhardt [8]. We start with the free Klein-Gordon field ϕ, which describes a (pseudo-) scalar i.e. spin-0 particle with mass m_ϕ. Its Lagrangian (of course in natural units $\hbar = c = 1$) is given by

$$\mathcal{L}_\phi = \frac{1}{2}\left[(\partial_\mu \phi)(\partial^\mu \phi) - m_\phi^2 \phi^2\right]. \tag{2.2}$$

For less confusion with indices, we colour Lorentz indices purple. The propagator of such a field is simply given by

$$\mathcal{P}_\phi(p) = \frac{\mathrm{i}}{p^2 - m_\phi^2 + \mathrm{i}\epsilon}. \tag{2.3}$$

Here and throughout the thesis we use the letter p to denote the four-momentum of a particle, ϵ is a real infinitesimal to avoid the singularity at $p^2 = m^2$. The Klein-Gordon field describes e.g. the pion, which we will introduce later on. However, the Klein-Gordon Lagrangian is helpful on our way to higher spin fields, such as the Dirac equation, which looks similar but is in first order. Its Lagrangian is given by

$$\mathcal{L}_\psi = \overline{\psi}(\partial\!\!\!/ - m_\psi)\psi, \tag{2.4}$$

where m is to be understood as a diagonal 4×4 matrix, $\partial\!\!\!/ = \gamma^\mu \partial_\mu$ is a convenient shorthand notation, $\overline{\psi} = \psi^\dagger \gamma^0$ and the anticommutator

$$\{\gamma^\mu, \gamma^\nu\} = 2\eta^{\mu\nu}\mathbb{1}_4 \tag{2.5}$$

gives a relation for the gamma matrices with the metric tensor $\eta^{\mu\nu} = \mathrm{diag}(1,-1,-1,-1)^{\mu\nu}$. We will also introduce another gamma matrix, which is the product of the four aforementioned ones and anticommutes with them:

$$\gamma^5 = \mathrm{i}\gamma^0\gamma^1\gamma^2\gamma^3 \qquad \{\gamma^5, \gamma^\mu\} = 0, \tag{2.6}$$

In Feynman diagrams incoming Dirac particles with spin s and mass m contribute with their spinor $u(p,s)$ ($v(p,s)$ for antiparticles) and outgoing particles with the conjugated spinors $\overline{u}(p,s)$, $\overline{v}(p,s)$ respectively. They obey the completeness relations

$$\sum_s u(p,s)\overline{u}(p,s) = p\!\!\!/ + m \qquad \sum_s v(p,s)\overline{v}(p,s) = p\!\!\!/ - m. \tag{2.7}$$

Multiplying the Klein-Gordon propagator Equation (2.3) with the completeness relation Equation (2.7) yields the Dirac propagator [9]

$$\mathcal{P}_\psi(p) = \frac{\mathrm{i}\left(p\!\!\!/ + m_\psi\right)}{p^2 - m_\psi^2 + \mathrm{i}\epsilon}. \tag{2.8}$$

Let us now consider a generic expression often found in the calculation of the invariant amplitude with arbitrary matrices $\Xi^{\mu\nu}$[10]:

$$|\mathcal{M}|^2 \propto \left[\overline{u}(p_f)_\alpha \Xi^{\alpha\beta} u(p_i)_\beta\right]\left[\overline{u}(p_f)_\mu \Xi^{\mu\nu} u(p_i)_\nu\right]^\dagger. \tag{2.9}$$

Note that we can write the Hermitian conjugate instead of the complex conjugate, since the expression in the square brackets is a scalar. Summing over the spins we can use the completeness relation, thus giving

$$\begin{aligned}\sum_{s,s'} |\mathcal{M}|^2 &\propto \sum_{s,s'}\left[\overline{u}^s_\alpha(p_f)\Xi^{\alpha\beta}u^{s'}_\beta(p_i)\right]\left[\overline{u}^{s'}_\mu(p_i)\overline{\Xi}^{\mu\nu}u^s_\nu(p_f)\right] \\ &= \Xi^{\alpha\beta}\left(p\!\!\!/_i + m_i\right)_{\beta\mu}\overline{\Xi}^{\mu\nu}\left(p\!\!\!/_f + m_f\right)_{\nu\alpha} \\ &= \mathcal{T}r\left\{\Xi\left(p\!\!\!/_i + m_i\right)\overline{\Xi}\left(p\!\!\!/_f + m_f\right)\right\},\end{aligned} \tag{2.10}$$

with $\overline{\Xi} = \gamma^0 \Xi^\dagger \gamma^0$. This allows us to drastically simplify the calculations as there are no spinors left. Now we only need to describe the photon field to be able to describe the decay process. The well known electromagnetic field is governed by the Lagrangian

$$\mathscr{L}_{\mathrm{EM}} = -\frac{1}{4}\mathcal{F}^{\mu\nu}\mathcal{F}_{\mu\nu}, \tag{2.11}$$

where

$$\mathcal{F}^{\mu\nu} = \partial^{[\mu}A^{\nu]} = \partial^{\mu}A^{\nu} - \partial^{\nu}A^{\mu} \tag{2.12}$$

is the electromagnetic field strength tensor and A^μ is the four-vector potential. It describes all massless spin-1 ((pseudo-) vector) particles. Adding a mass term leads to the Proca field B^μ, which describes for example the ρ

$$\mathscr{L}_B = -\frac{1}{4}\mathcal{G}^{\mu\nu}\mathcal{G}_{\mu\nu} + \frac{1}{2}m_B^2 B^\mu B_\mu, \tag{2.13}$$

where $\mathcal{G}^{\mu\nu} = \partial^{[\mu}B^{\nu]}$. Finally all we need is to describe the interaction between the photon gauge field and the Dirac field, which we get by replacing the partial derivative in Equation (2.4) with the covariant gauge derivative

$$\partial_\mu \to \mathcal{D}_\mu = \partial_\mu + \mathrm{i}eA_\mu, \tag{2.14}$$

where e is the coupling constant for the electromagnetic field. This leads to the interaction term

$$\mathscr{L}_{\gamma ee} = \mathrm{i}e\overline{\psi}_e \gamma^\mu A_\mu \psi_e. \tag{2.15}$$

2.2 Polarisation Vectors

The spin-1 fields contribute with their polarisation vector $\epsilon_\mu(p,\lambda)$ for incoming and $\epsilon^*_\mu(p,\lambda)$ for outgoing particles. Here λ is the helicity of particle, which is the projection of its spin on the direction of motion. This formalism allows for a relativistic treatment of angular momentum and spin, which are both defined in different frames of reference. The helicity however is invariant under rotations and boosts that don't "overtake" the particle. We therefore use the helicity to parametrise a basis of eigenstates. For a massive spin-1 particle, its helicity can assign one of the three eigenvalues $\lambda \in \{-1, 0, 1\}$. An eigenvalue of -1 corresponds to a left-handed circularly polarised state, $+1$ for the right-handed one and $\lambda = 0$ for a longitudinal polarised state. However, in the four-vector formalism there are four components, thus the field has an additional, unphysical degree of freedom (DoF). We can eliminate this extra degree by imposing the Lorenz condition, i.e. $\partial_\mu \epsilon^\mu = 0$. The polarisation vectors are normalised

$$\epsilon^\mu(p,\lambda)\epsilon^*_\mu(p,\lambda') = -\delta_{\lambda\lambda'}, \tag{2.16}$$

and transversal to p

$$\epsilon^\mu(p,\lambda)p_\mu = 0. \tag{2.17}$$

The completeness relation for the polarisation vectors is given by

$$\sum_{\lambda=\pm1,0} \epsilon^\mu(p,\lambda)\epsilon^{*\nu}(p,\lambda) = -\eta^{\mu\nu} + \frac{p^\mu p^\nu}{p^2}. \tag{2.18}$$

Hence, the propagator for a massive particle is given by

$$\mathcal{P}^{\mu\nu}{}_B(p) = \frac{-\mathrm{i}\left(\eta^{\mu\nu} - \frac{p^\mu p^\nu}{p^2}\right)}{p^2 - m_B^2 + \mathrm{i}\epsilon}. \tag{2.19}$$

The massless propagator takes a more complicated form. However, in our case, we take note, that the vertices will be orthogonal to the momenta, thus Equation (2.19) simplifies to

$$\mathcal{P}^{\mu\nu}{}_B(p) = \frac{-i\eta^{\mu\nu}}{p^2 - m_B^2 + i\epsilon}, \tag{2.20}$$

which in the massless case becomes

$$\mathcal{P}^{\mu\nu}{}_A(p) = \frac{-i\eta^{\mu\nu}}{p^2 + i\epsilon}. \tag{2.21}$$

For a more rigorous version that of course will conclude the same result, see for example [**needed**].

2.3 Decay Matrix

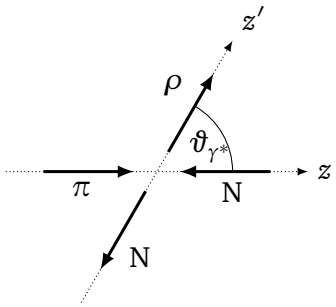

Figure 2.3.: Kinematics of the $\pi N \to \rho N$ reaction in the CM frame

Now, we can write down the decay matrix element for Figure 2.2 as

$$\mathcal{M}^{\text{decay}}(\lambda) = ie\mathcal{L}^{\mu}\epsilon_{\mu}(\lambda), \tag{2.22}$$

with

$$\mathcal{L}^{\mu} = ie\bar{u}(p^-, s^-)\gamma^{\mu}v(p^+, s^+). \tag{2.23}$$

Squaring this yields

$$\mathcal{M}^{\text{decay}}\mathcal{M}^{\text{decay}*} = -e^2\mathcal{L}^{\mu}\epsilon_{\mu}(\lambda)\epsilon^*_{\nu}(\lambda)\mathcal{L}^{*\nu}. \tag{2.24}$$

We now define the lepton tensor as the sum of the leptonic interaction over the electron spins

$$\mathcal{L}^{\mu\nu} = \sum_{s^+s^-} \mathcal{L}^{\mu}\mathcal{L}^{*\nu}, \tag{2.25}$$

and the spin density matrix for the decay

$$\rho^{\text{decay}}_{\lambda\lambda'} = \epsilon^*_{\mu}(\lambda)\mathcal{L}^{\mu\nu}\epsilon_{\nu}(\lambda'). \tag{2.26}$$

By using the completeness relation Equation (2.7) and employing Casimir's Trick Equation (2.10), we can express the spin sum over the squared matrix element as a trace over the gamma matrices which after another short calculation yields

$$\sum_{s^+s^-} \left|\mathcal{M}^{\text{decay}}\right|^2 = 4e^2\left[p^+_{\mu}p^-_{\nu} + p^+_{\nu}p^-_{\mu} - (p^+ \cdot p^-)\eta_{\mu\nu}\right], \tag{2.27}$$

where we used the ultrarelativistic limit $m \ll q$. Since the actual photon in the process is virtual, we choose the rest frame of the photon as our frame of reference. Using spherical coordinates the momenta of the leptons are given by

$$p^{\pm} = q \begin{pmatrix} 1 \\ \pm \sin\vartheta \cos\varphi \\ \pm \sin\vartheta \sin\varphi \\ \pm \cos\vartheta \end{pmatrix}, \tag{2.28}$$

where the angles are measured between the quantisation axis of the photon and the three momentum direction of the leptons; and q is the modulus of the three-momentum. We choose the spin quantisation axis to canonically coincide with the z'-axis as seen in Figure 2.3. The polarisation vectors from Section 2.2 then take the explicit form

$$\begin{aligned} \epsilon^{\mu}(p,-1) &= \frac{1}{\sqrt{2}}(0,1,-\mathrm{i},0)^{\mu}, \\ \epsilon^{\mu}(p,+1) &= \frac{-1}{\sqrt{2}}(0,1,\mathrm{i},0)^{\mu}, \\ \epsilon^{\mu}(p,0) &= (0,0,0,1)^{\mu}, \end{aligned} \tag{2.29}$$

where the axes were defined before boosting to the rest frame. This allows us to explicitly calculate the decay matrix, for which the indices of the rows and columns range over the helicity from -1 to $+1$

$$\rho^{\mathrm{decay}}_{\lambda'\lambda} = \frac{1}{2} \begin{pmatrix} L_{11}+L_{22} & \sqrt{2}(L_{13}+\mathrm{i}L_{23}) & -L_{11}-2\mathrm{i}L_{21}+L_{22} \\ \sqrt{2}(L_{13}-\mathrm{i}L_{23}) & 2L_{33} & -\sqrt{2}(L_{13}+\mathrm{i}L_{23}) \\ -L_{11}+2\mathrm{i}L_{21}+L_{22} & -\sqrt{2}(L_{13}-\mathrm{i}L_{23}) & L_{11}+L_{22} \end{pmatrix}_{\lambda'\lambda}. \tag{2.30}$$

We see, that by definition, this matrix is hermitian i.e. $\rho^{\mathrm{decay}} = \rho^{\mathrm{decay}^{\dagger}}$. Plugging in the lepton tensor, we find:

$$\rho^{\mathrm{decay}}_{\lambda'\lambda} = 4q^2 \begin{pmatrix} 1+\cos^2\vartheta & -\frac{2}{\sqrt{2}}e^{\mathrm{i}\varphi}\sin 2\vartheta & e^{2\mathrm{i}\varphi}\sin^2\vartheta \\ -\frac{\sqrt{2}}{2}e^{-\mathrm{i}\varphi}\sin 2\vartheta & 2(1-\cos^2\vartheta) & \frac{2}{\sqrt{2}}e^{\mathrm{i}\varphi}\sin 2\vartheta \\ e^{-2\mathrm{i}\varphi}\sin^2\vartheta & \frac{2}{\sqrt{2}}e^{-\mathrm{i}\varphi}\sin 2\vartheta & 1+cos^2\vartheta \end{pmatrix}_{\lambda'\lambda}. \tag{2.31}$$

2.4 Anisotropy Coefficients

We now proceed analogously to the decay matrix for the production matrix

$$\mathcal{M}^{\mathrm{prod}} = \epsilon^{*}_{\mu}\mathcal{H}^{\mu}. \tag{2.32}$$

We are not concerned with the explicit form of $\mathcal{H}^{\mu}$ at this point. This will be discussed in the following sections. Similiarly to Equation (2.25) and Equation (2.26) we define

$$\begin{aligned} \mathcal{H}^{\mu\nu} &= \sum_{\mathrm{spins}} \mathcal{H}^{\mu}\mathcal{H}^{*\nu} \\ \rho^{\mathrm{decay}}_{\lambda\lambda'} &= \epsilon^{*}_{\mu}(\lambda)\mathcal{H}^{\mu\nu}\epsilon_{\nu}(\lambda'). \end{aligned} \tag{2.33}$$

The total matrix element is given by

$$\mathcal{M} = \sum_{\lambda} \mathcal{M}^{\mathrm{decay}}(\lambda)\mathcal{M}^{\mathrm{prod}}(\lambda). \tag{2.34}$$

Plugging in the individual amplitudes, squaring and summing gives

$$\sum_{\text{spins}} |\mathcal{M}|^2 = \sum_{\text{spins}} \sum_{\lambda,\lambda'} \mathcal{L}^{\mu} \epsilon(\lambda)_{\mu} \epsilon^*_{\nu}(\lambda) \mathcal{H}^{\nu} \mathcal{H}^{*\nu'} \epsilon_{\nu'}(\lambda') \epsilon^*(\lambda')_{\mu'} \mathcal{L}^{*\mu'}. \tag{2.35}$$

With Equation (2.26) and Equation (2.33) we get

$$\sum_{\text{spins}} |\mathcal{M}|^2 = \sum_{\lambda,\lambda'} \rho^{\text{decay}}_{\lambda'\lambda} \rho^{\text{prod}}_{\lambda\lambda'}. \tag{2.36}$$

With Equation (2.36) we can give a relation for $|\mathcal{M}|^2$ which only depends on the elements of the production spin density matrix

$$\begin{aligned} |\mathcal{M}|^2 \propto\ & (1+\cos^2\vartheta)(\rho^{\text{prod}}_{-1,-1} + \rho^{\text{prod}}_{+1,+1}) + 2(1-\cos^2\vartheta)\rho^{\text{prod}}_{0,0} \\ & + \frac{\sqrt{2}}{2} \sin 2\vartheta \left[e^{-\mathrm{i}\varphi} \left(\rho^{\text{prod}}_{0,+1} - \rho^{\text{prod}}_{-1,0} \right) + e^{\mathrm{i}\varphi} \left(\rho^{\text{prod}}_{0,1} - \rho^{\text{prod}}_{-1,0} \right)^* \right] \\ & + \sin^2\vartheta (e^{-2\mathrm{i}\varphi} \rho^{\text{prod}} + e^{2\mathrm{i}\varphi} \rho^{\text{prod}\ *}_{-1,+1}). \end{aligned} \tag{2.37}$$

We can now introduce the anisotropy coefficients λ, which restructure Equation (2.37)

$$\begin{aligned} |\mathcal{M}|^2 \propto \mathcal{N} \Big(& 1 + \lambda_\vartheta \cos^2\vartheta + \lambda_\varphi \sin^2\vartheta \cos 2\varphi + \lambda_{\vartheta\varphi} \sin 2\vartheta \cos\varphi \\ & + \lambda^{\perp}_{\varphi} \sin^2\vartheta \sin 2\varphi + \lambda^{\perp}_{\varphi} \lambda_{\vartheta\varphi} \sin 2\vartheta \sin\varphi \Big). \end{aligned} \tag{2.38}$$

The coefficients are

$$\lambda_\vartheta = \frac{1}{\mathcal{N}} \left(\rho^{\text{prod}}_{-1,-1} + \rho^{\text{prod}}_{+1,+1} - 2\rho^{\text{prod}}_{0,0} \right), \tag{2.39}$$

$$\lambda_\varphi = 2\frac{1}{\mathcal{N}} \mathcal{R}e \left(\rho^{\text{prod}}_{-1,+1} \right), \tag{2.40}$$

$$\lambda_{\vartheta\varphi} = \frac{\sqrt{2}}{\mathcal{N}} \mathcal{R}e \left(\rho^{\text{prod}}_{0,+1} - \rho^{\text{prod}}_{-1,0} \right), \tag{2.41}$$

$$\lambda^{\perp}_{\varphi} = \frac{2}{\mathcal{N}} Im \left(\rho^{\text{prod}}_{-1,+1} \right), \tag{2.42}$$

$$\lambda^{\perp}_{\vartheta\varphi} = \frac{\sqrt{2}}{\mathcal{N}} Im \left(\rho^{\text{prod}}_{0,+1} - \rho^{\text{prod}}_{-1,0} \right), \tag{2.43}$$

with the normalisation constant

$$\mathcal{N} = \rho^{\text{prod}}_{-1,-1} + \rho^{\text{prod}}_{+1,+1} + 2\rho^{\text{prod}}_{0,0}. \tag{2.44}$$

As Speranza[2] has noted, $\lambda^{\perp}_{\varphi}$ and $\lambda^{\perp}_{\vartheta\varphi}$ violate reflection symmetry but not parity. Note that the differential cross section

$$\frac{\partial\sigma}{\partial\Omega} \propto \sum |\mathcal{M}|^2. \tag{2.45}$$

Integrating Equation (2.38) over φ leaves us with

$$\int_0^{2\pi} \sum_{\text{spins}} |\mathcal{M}|^2 \, \mathrm{d}\varphi \propto 2\pi\mathcal{N} \left(1 + \lambda_\vartheta \cos^2\vartheta \right). \tag{2.46}$$

We find that the φ terms do not contribute to the total cross section. Introducing the transverse polarisation of the intermediate particle $\Sigma_\perp = \rho^{\text{prod}}_{-1,-1} + \rho^{\text{prod}}_{+1,1}$ and the parallel one $\Sigma_\parallel = 2\rho^{\text{prod}}_{0,0}$, Equation (2.46) takes the form

$$\int_0^{2\pi} \sum_{\text{spins}} |\mathcal{M}|^2 \, \mathrm{d}\varphi \propto 2\pi\mathcal{N}\left(\Sigma_\perp(1+\cos^2\vartheta) + \Sigma_\parallel(1-\cos^2\vartheta)\right). \tag{2.47}$$

Comparing Equation (2.46) with Equation (2.47) we get

$$\lambda_\vartheta = \frac{\Sigma_\perp - \Sigma_\parallel}{\Sigma_\perp + \Sigma_\parallel}. \tag{2.48}$$

Note that this only holds true for massless particles, which we assume for the dilepton pair since $m_e \ll q$. The interpretation of the anisotropy now becomes clear, as $\lambda_\vartheta = -1$ for a completely parallel polarised particle $\Sigma_\perp = 0$. Likewise $\lambda_\vartheta = +1$ for a completely transversally polarised particle $\Sigma_\parallel = 0$. Finally we want to point out, that the anisotropy coefficient is not frame independent. We formulated 2.38 in the rest frame of the virtual photon, where we chose a quantisation axis. However, the choice is arbitrary. We choose the helicity frame, whose quantisation axis coincides with the direction of momentum of the photon. Note that by switching to another frame, the other anisotropy coefficients do not necessarily vanish.

2.5 Isospin

We now come to the more complex part, in which the photon is produced. Not every combination of incoming pions and nucleons is allowed, since isospin needs to be conserved in strong interactions. The fact that the strong force acts equally on a proton and a neutron and both particles' nearly identical mass allow us to introduce isospin as an additional symmetry and regard them as different states of one particle - the nucleon. The nucleon is a composite particle that consists of a combination of three up and down quarks in total. Canonically we choose the quantisation axis along the z-axis and assign the up-quark an isospin of $I_z = +1/2$ and consequently the down-quark an isospin of $I_z = -1/2$. From there follows the isospin for the nucleon doublet

$$\begin{aligned} |p\rangle &= |I = 1/2, I_z = +1/2\rangle = \begin{pmatrix} 1 \\ 0 \end{pmatrix} \\ |n\rangle &= |I = 1/2, I_z = -1/2\rangle = \begin{pmatrix} 0 \\ 1 \end{pmatrix}. \end{aligned} \tag{2.49}$$

Isospin can be described by $\mathcal{SU}(2)$ symmetry, whose generators are given by the Pauli matrices

$$\tau_1 = \begin{pmatrix} 0 & 1 \\ 1 & 0 \end{pmatrix} \qquad \tau_2 = \begin{pmatrix} 0 & \mathrm{i} \\ -\mathrm{i} & 0 \end{pmatrix} \qquad \tau_3 = \begin{pmatrix} 1 & 0 \\ 0 & -1 \end{pmatrix}. \tag{2.50}$$

To look at mesons which consists of two isospin-1/2 particles we have to look at the direct product of the $\mathcal{SU}(2)$ representation. We find that $2 \otimes 2 = 3 \oplus 1$, which means we have a triplet and a singlet state. The basis states of the triplet are simply given by

$$\pi^1 = \begin{pmatrix} 1 \\ 0 \\ 0 \end{pmatrix}, \quad \pi^2 = \begin{pmatrix} 0 \\ 1 \\ 0 \end{pmatrix}, \quad \pi^3 = \begin{pmatrix} 0 \\ 0 \\ 1 \end{pmatrix}, \tag{2.51}$$

and are often grouped as a vector $\vec{\pi} = (\pi^1 \quad \pi^2 \quad \pi^3)^{\mathrm{T}}$. From here on we will refer to isospin indices in green colour for clarity. These basis states form the three pions which consist of two charged ones, which

are all eigenstates for rotations around the z-axis. (The isospin quantisation axis was chosen to coincide with the z-axis). Thus,

$$\pi^{\pm} = \frac{1}{\sqrt{2}}(\pi^1 \mp i\pi^2), \quad \pi^0 = \pi^3. \tag{2.52}$$

Likewise, expressing the isospin components in terms of the physical fields yields

$$\begin{aligned} \pi^1 &= \frac{1}{\sqrt{2}}(\pi^+ + \pi^-) \\ \pi^2 &= \frac{1}{i\sqrt{2}}(\pi^+ - \pi^-). \end{aligned} \tag{2.53}$$

For particles like the Δ-baryon with isospin 3/2, this formalism has yet to be extended. Following $2 \otimes 2 \otimes 2 = 4 \oplus 2 \oplus 2$ we identify the Δ-baryon as the quadruplet. Its isospin basis states are clearly of dimension 1×4, thus we need special transition matrices to couple a Δ-baryon to an isospin 1/2 particle like the nucleon. This transition matrices were derived in [11] and are given by

$$T_1 = \begin{pmatrix} -\sqrt{\frac{1}{2}} & 0 \\ 0 & -\sqrt{\frac{1}{6}} \\ \sqrt{\frac{1}{6}} & 0 \\ 0 & \sqrt{\frac{1}{2}} \end{pmatrix} \qquad T_2 = \begin{pmatrix} i\sqrt{\frac{1}{2}} & 0 \\ 0 & i\sqrt{\frac{1}{6}} \\ i\sqrt{\frac{1}{6}} & 0 \\ 0 & i\sqrt{\frac{1}{2}} \end{pmatrix} \qquad T_3 = \begin{pmatrix} 0 & 0 \\ \sqrt{\frac{2}{3}} & 0 \\ 0 & \sqrt{\frac{2}{3}} \\ 0 & 0 \end{pmatrix} \tag{2.54}$$

2.6 Vector Meson Dominance

To couple the leptonic with the hadronic part of the process, we must focus on the electromagnetic interaction of hadrons. Early measurements have shown, that the interaction between photons and hadrons is more intense than what a direct interaction would predict. Vector Meson Dominance (VMD) is the most commonly used model to account for the difference [2]. Sakurai was the first to propose the idea that photons couple to hadrons through the exchange of vector mesons (VMD1) [12, 13]. This idea was later refined by Kroll, Lee, and Zumino [14] in order to make it gauge invariant. Following the convention of Bjorken and Drell [15], the Lagrangian describing ρ-mesons and pions is given by

$$\mathcal{L} = -\frac{1}{4}\vec{\rho}_{\mu\nu}\vec{\rho}^{\mu\nu} + \frac{1}{2}m_\rho^2\vec{\rho}_\mu\vec{\rho}^\mu + \frac{1}{2}D_\mu\vec{\pi}\cdot D^\mu\vec{\pi} - \frac{1}{2}m_\pi^2\vec{\pi}\cdot\vec{\pi}, \tag{2.55}$$

where $\vec{\rho}$ and $\vec{\pi}$ are the isovector fields of the respective mesons and $m_{\rho/\pi}$ are their respective masses. Also

$$D_\mu\vec{\pi} = \partial_\mu\vec{\pi} - g_{\rho\pi\pi}\vec{\rho}_\mu \times \vec{\pi} \tag{2.56}$$

is the covariant derivative which gives rise to the interaction term. As we are only concerned with the neutral ρ-meson, only the third component of the ρ-field contributes to the interaction. Plugging Equation (2.56) into Equation (2.55), we find the pion kinetic term and its interaction with ρ-mesons plus a four point interaction quadratic in g

$$\mathcal{L} = \frac{1}{2}D_\mu\vec{\pi}\cdot D^\mu\vec{\pi} = \frac{1}{2}(\partial_\mu\vec{\pi})(\partial^\mu\vec{\pi}) + g(\partial^\mu\vec{\pi})\cdot(\vec{\rho}_\mu\times\vec{\pi}) + \frac{g^2}{2}(\vec{\rho}_\mu\times\vec{\pi})(\vec{\rho}^\mu\times\vec{\pi}). \tag{2.57}$$

The middle term is the desired interaction Lagrangian. We permute the parallelepipedial product cyclically and rewrite the vector product so we find its dependence on the isospin components of the respective fields

$$\mathcal{L}_{\rho\pi\pi} = g\epsilon_{abc}\pi^a(\partial^\mu\pi^b)\rho_\mu{}^c. \tag{2.58}$$

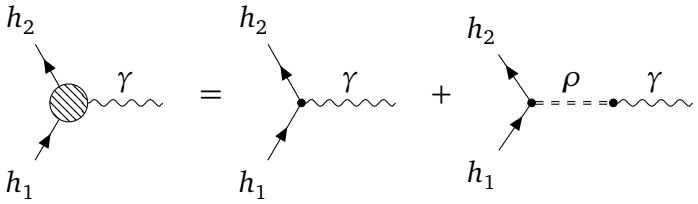

Figure 2.4.: The interaction between the photon and two generic hadrons according to the VMD2.

To find the interaction between the physical fields, we use Equation (2.53). Since we are only concerned with the neutral ρ meson we let $c = 3$ because $\rho^0 = \rho^3$. We then find

$$\begin{aligned}
\mathscr{L}_{\text{int}} &= g_{\rho\pi\pi}\left[\pi^1(\partial^\mu\pi^2) - \pi^2(\partial^\mu\pi^1)\right]\rho^3{}_\mu \\
&= \frac{-\mathrm{i}g_{\rho\pi\pi}}{2}\left[(\pi^+ + \pi^-)\partial^\mu(\pi^+ - \pi^-) - (\pi^+ - \pi^-)\partial^\mu(\pi^+ + \pi^-)\right]\rho^0_\mu \\
&= -\mathrm{i}g_{\rho\pi\pi}\left[\pi^-(\partial^\mu\pi^+) - \pi^+(\partial^\mu\pi^-)\right]\rho^0_\mu \\
&= -g_{\rho\pi\pi}J^\mu{}_\pi\rho^0_\mu,
\end{aligned} \tag{2.59}$$

where J_π is the pion current. Note that the ρ-meson must not decay into two neutral pions, which is taken care of by the vector product. The first idea of Sakurai assumed, that the hadronic electromagnetic current operator is proportional to the vector meson field, resulting in the interaction Lagrangian

$$\mathscr{L}^1_{\rho\gamma} = -\frac{em_\rho^2}{g_\rho}\rho^0_\mu A^\mu. \tag{2.60}$$

But this Lagrangian is not gauge invariant, thus we cannot add it to Equation (2.55). Instead, we will use the Lagrangian proposed by Kroll et al., which, by construction, is gauge invariant:

$$\mathscr{L}^2_{\rho\gamma} = -\frac{e}{2g_\rho}F^{\mu\nu}\rho^0_{\mu\nu}. \tag{2.61}$$

However, by rewriting it in momentum space and using Equation (2.17)

$$\mathscr{L}^2_{\rho\gamma} = -\frac{e}{g_\rho}p^2A^\mu\rho_\mu, \tag{2.62}$$

we find that the interaction vanishes for $p^2 = 0$, e.g. real photons. Therefore, another term for direct photon coupling is needed in this version of VMD (see Figure 2.4). This leaves us with the total Lagrangians

$$\begin{aligned}
\mathscr{L}^1 &= -e\frac{m_\rho^2}{g_\rho}\rho^0_\mu A^\mu - g_{\rho\pi\pi}\rho^0_\mu J^\mu \\
\mathscr{L}^2 &= \frac{e}{2g_\rho}F^{\mu\nu}\rho^0_{\mu\nu} - eJ_\mu A^\mu - g_{\rho\pi\pi}\rho^0_\mu J^\mu.
\end{aligned} \tag{2.63}$$

Using these we can now calculate the pion form factor, by regarding the transition $\gamma \to \pi^+\pi^-$. The

matrix elements are given by

$$\begin{aligned}
\mathcal{M}^1_{\gamma\to\pi\pi} &= g_{\rho\pi\pi}(p_{\pi^+}-p_{\pi^-})^\mu \frac{\eta_{\mu\nu}}{p_\rho^2-m_\rho^2}\frac{em_\rho^2}{g_\rho}\eta^{\nu\xi}\epsilon_{\gamma,\xi} \\
&= -e(p_{\pi^+}-p_{\pi^-})^\mu \epsilon_{\gamma,\mu} F_\pi^1(p_\rho^2) \\
\mathcal{M}^2_{\gamma\to\pi\pi} &= e(p_{\pi^+}-p_{\pi^-})^\mu \left(-\epsilon_{\gamma,\mu} + g_{\rho\pi\pi}\frac{\eta_{\mu\nu}}{p_\rho^2-m_\rho^2}\frac{em_\rho^2}{g_\rho}\eta^{\nu\xi}\epsilon_{\gamma,\xi}\right) \\
&= -e(p_{\pi^+}-p_{\pi^-})^\mu \epsilon_{\gamma,\mu} F_\pi^2(p_\rho^2)
\end{aligned} \tag{2.64}$$

From there we can read off the pion form factor, which gives the deviation from a point-like interaction:

$$\begin{aligned}
F_\pi^1(p_\pi^2) &= -\frac{m_\rho^2}{p_\rho^2-m_\rho^2}\frac{g_{\rho\pi\pi}}{g_\rho} \\
F_\pi^2(p_\pi^2) &= 1-\frac{p_\rho^2}{p_\rho^2-m_\rho^2}\frac{g_{\rho\pi\pi}}{g_\rho}
\end{aligned} \tag{2.65}$$

For zero momentum transfer the pion "sees" the interaction as point-like, therefore $F_\pi(0)=1$. In VMD2 this is immediately apparent, while in VMD1 we have to demand $g_{\rho\pi\pi}=g_\rho$, which leads to the argument of universal couplings, i.e. the coupling of the ρ-meson is the same with all particles. In this thesis we will use VMD2 to describe the coupling between hadrons and photons. This allows us to have more control over the coupling constants, because we can fix them independently (for photon and ρ-meson coupling).

2.7 Relativistic QFT II: Rarita-Schwinger-Field and Consistent Couplings

This section is based on the work of Pascalutsa [16] [17]. Higher spin fields need additional degrees of freedom compared to the Dirac field. We therefor introduce the Rarita-Schwinger equation for a spin-3/2 particle with mass m (note that also a general version for spin-$n/2$ particles exists)

$$\mathcal{L} = \overline{\psi}_\mu \Lambda^{\mu\nu}\psi^\nu, \tag{2.66}$$

where

$$\begin{aligned}
\Lambda^{\mu\nu} &= \mathrm{i}\gamma^{\mu\nu\alpha}\partial_\alpha - m\gamma^{\mu\nu} \\
\gamma^{\mu\nu} &= \frac{1}{2}[\gamma^\mu,\gamma^\nu] \\
\gamma^{\mu\nu\alpha} &= \frac{1}{2}\{\gamma^{\mu\nu},\gamma^\alpha\}.
\end{aligned} \tag{2.67}$$

The corresponding field equations are given by

$$\Lambda^{\mu\nu}\psi_\nu = 0 = \gamma_\mu\Lambda^{\mu\nu}\psi_\nu = \partial_\mu\Lambda^{\mu\nu}\psi_\nu. \tag{2.68}$$

A Rarita-Schwinger vector-spinor ψ_μ has 16 components, but only needs $(2s+1)=4$ to describe its spin states. It can be concluded, that the remaining components contribute to the lower spin background. For free particles this is attuned with the constraints in Equation (2.68), which eliminate the unphysical DoF. However, in the interaction case we may have non-trivial couplings which make the treatment of the lower spin background more complex. This can lead to a difference in the number of DoF for the free

and interacting particle and as such make the theory inconsistent. The kinetic term is invariant under the gauge transformation

$$\psi_\mu \to \psi_\mu + \partial_\mu \epsilon \tag{2.69}$$

up to a total derivative, with ϵ being a spinor. We now consider a linear coupling of the form

$$\mathscr{L}_{\text{int}} = g\overline{\psi}_\mu j^\mu + \text{h.c.}, \tag{2.70}$$

where g is a coupling constant and j^μ is a current that may depend on other fields than ψ. To be consistent with the free theory i.e. invariant under Equation (2.69), j^μ has to be divergenceless i.e. $\partial_\mu j^\mu = 0$. Thus any interaction with a non conserved current violates DoF counting. Pascalutsa has shown that a redefinition of the Rarita-Schwinger field can make any inconsistent interaction consistent. For a detailed derivation see [16] [17]. We can guarantee a consistent interaction by replacing $\psi_\mu \to \Psi_\mu$, with

$$\Psi_\mu = \mathrm{i}\gamma^\nu \partial_{[\mu}\psi_{\nu]}. \tag{2.71}$$

The general propagator for a 3/2-spin particle is given by

$$\mathcal{P}_\Psi^{\mu\nu}(p) = \frac{\mathrm{i}P^{\mu\nu}}{p^2 - m^2}, \tag{2.72}$$

where

$$P^{\mu\nu}(p) = -(\not{p} + m)\left(\eta^{\mu\nu} - \frac{\gamma^\mu\gamma^\nu}{3} - \frac{2p^\mu p^\nu}{3m^2} + \frac{p^{[\mu}\gamma^{\nu]}}{3m}\right), \tag{2.73}$$

which in our case simplifies to

$$P^{\mu\nu}(p) = -(\not{p} + m)\left(\eta^{\mu\nu} - \frac{\gamma^\mu\gamma^{nu}}{3}\right). \tag{2.74}$$

2.8 Propagator Dressing

The propagators we have given are all for free, non interacting particles. However, in our case, the intermediate particles can interact and therefore we have to consider these deviations from the free (bare) propagator. By dressing the propagator, we take various processes into account (see for example Figure 2.5). For the ρ we will simply use its decay width

$$\mathcal{P}_\rho(p) \propto \frac{1}{p^2 - m_\rho^2 + \mathrm{i}\Gamma_\rho^2}. \tag{2.75}$$

For the nucleon resonance we use the parametrization of the width as in [18]

$$\mathcal{P}_{\text{R}}(p) \propto \frac{1}{p^2 - m_R^2 + \sqrt{p^2}\Gamma_{\text{R}}(p^2)}, \tag{2.76}$$

where

$$\Gamma_{\text{R}}(p^2) = \Gamma(m_{\text{R}}^2)\frac{m_{\text{R}}}{\sqrt{p^2}}\left(\frac{q}{q_{\text{R}}}\right)^{2l+1}\left(\frac{q_{\text{R}}^2 + \delta^2)}{q^2 + \delta^2}\right)^{l+1}. \tag{2.77}$$

The angular momentum of the pion is given by l, q denotes the incoming momentum of the pion for the off-shell resonance while q_R is the same quantity for an on-shell resonance. The cutoff parameter is given by

$$\delta^2 = (m_{\text{R}} - m_{\text{N}} - m_\pi)^2 + \frac{\Gamma^2(m_{\text{R}}^2)}{4} \tag{2.78}$$

We will not dress the virtual photon, as we expect the QED correction to be fairly small.

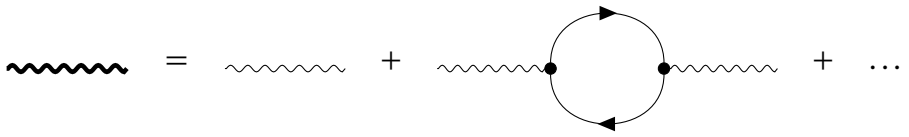

Figure 2.5.: Scheme for propagator dressing. The dressed propagator is the sum of the bare propagator and self interacting terms.

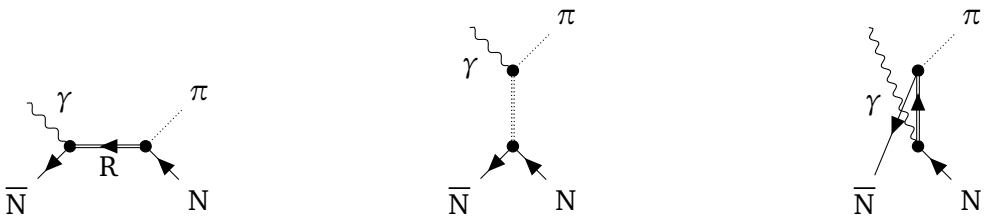

Figure 2.6.: Possible processes for $\pi N \to N\gamma$. $\overline{N}$ denotes the outgoing nucleon.

2.9 Interactions

The hadronic part can be divided in three channels s, t and u, distinguished by the momentum transport. For the process $\pi, N \to \gamma, \overline{N}$, where $\overline{N}$ denotes the outgoing nucleon, these are shown in Figure 2.6 and given by

$$\begin{aligned} s &= (p_\pi + p_N)^2 = (p_{\overline{N}} + p_\gamma)^2 \\ t &= (p_\pi - p_\gamma)^2 = (p_N - p_{\overline{N}})^2 \\ u &= (p_\pi - p_{\overline{N}})^2 = (p_\gamma - p_N)^2. \end{aligned} \tag{2.79}$$

We find the same type of interactions for the s- and u- channel, where we will only focus on resonant contributions, not considering the Born terms. The interaction Lagrangians are taken from Zétényi and Wolf [18] and were derived in an effective field theory approach. The derivation of the corresponding Feynman rules is shown in Appendix A. Here and thereafter $\Gamma = \gamma^5$ for resonances with $J^P \in \{1/2^+, 3/2^-\}$ and $\Gamma = 1$ otherwise, and $\tilde{\Gamma} = \gamma^5\Gamma$. We find the following interactions for the γNR, ρNR and πNR vertices:

$$\mathcal{L}_{\rho \mathrm{NR}_{1/2}} = \frac{g_{\rho \mathrm{NR}}}{2m_\rho} \overline{\psi}_R \vec{\tau} \sigma^{\mu\nu} \tilde{\Gamma} \Psi_N \cdot \vec{\rho}_{\mu\nu} + \mathrm{h.c.}, \tag{2.80}$$

$$\mathcal{L}_{\rho \mathrm{NR}_{3/2}} = -\mathrm{i} \frac{g_{\rho \mathrm{NR}}}{m_\rho} \overline{\psi}^\mu_R \vec{\mathcal{T}} \gamma^\nu \tilde{\Gamma} \psi_N \cdot \vec{\rho}_{\mu\nu} + \mathrm{h.c.}, \tag{2.81}$$

$$\mathcal{L}_{\gamma \mathrm{NR}_{1/2}} = \frac{g_{\rho \mathrm{NR}}}{2m_\rho} \overline{\psi}_R \sigma^{\mu\nu} \tilde{\Gamma} \Psi_N \mathcal{F}_{\mu\nu} + \mathrm{h.c.}, \tag{2.82}$$

$$\mathcal{L}_{\gamma \mathrm{NR}_{3/2}} = -\mathrm{i} \frac{g_{\rho \mathrm{NR}}}{m_\rho} \overline{\psi}^\mu_R \gamma^\nu \tilde{\Gamma} \psi_N \mathcal{F}_{\mu\nu} + \mathrm{h.c.}, \tag{2.83}$$

$$\mathcal{L}_{\pi \mathrm{NR}_{1/2}} = -\frac{g_{\pi \mathrm{NR}}}{m_\pi} \overline{\psi}_R \Gamma \gamma^\mu \vec{\tau} \psi_N \cdot \partial_\mu \vec{\pi} + \mathrm{h.c.}, \tag{2.84}$$

$$\mathcal{L}_{\pi \mathrm{NR}_{3/2}} = \frac{g_{\pi \mathrm{NR}}}{m_\pi} \overline{\psi}^\mu_R \Gamma \vec{\mathcal{T}} \psi_N \cdot \partial_\mu \vec{\pi} + \mathrm{h.c.}. \tag{2.85}$$

Here pseudo-vector ($\Gamma\gamma^\mu$) couplings are employed in the case of spin-1/2 resonances. $\vec{\mathcal{T}} = \vec{\tau}$ for $R = N^*$ and $\vec{\mathcal{T}} = \vec{T}$ for $R = \Delta$. The isospin structure accounts for all possible processes of $N\pi \to N\rho^0$, which easily can be seen. Let's consider the processes

$$\begin{aligned} &1) \quad n\pi^0 \to n^* \to n\rho^0 \\ &2) \quad n\pi^0 \to n^* \to p\rho^0. \end{aligned}$$

Clearly the second process is forbidden for charge and isospin conservation reasons. Plugging in the isospin indices into Equation (2.80) and Equation (2.84) we find

$$\mathcal{M}^1 \propto \tau^3{}_{22}\tau^3{}_{22} = (-1)^2 \tag{2.86}$$
$$\mathcal{M}^2 \propto \tau^3{}_{22}\tau^3{}_{21} = 0, \tag{2.87}$$

thus the second process is indeed forbidden by the interaction Lagrangians. When deriving the Feynman rules one has to consider the spin consistency transformation Equation (2.71) for the higher spin-case. The following interactions are found in the t-channel [18]:

$$\mathcal{L}_{\pi NN} = -\frac{g_{\pi NN}}{m_\pi}\overline{\psi}_N\gamma^5\gamma^\mu\vec{\tau}\psi_N \cdot \partial_\mu\vec{\pi} \tag{2.88}$$
$$\mathcal{L}_{\rho NN} = \frac{g_\rho}{2}\overline{\psi}_N\left(\vec{\phi} - \kappa_\rho\frac{\sigma_{\mu\nu}}{4m_N}\vec{\rho}^{\mu\nu}\right)\cdot\vec{\tau}\psi_N \tag{2.89}$$
$$\mathcal{L}_{a_1 NN} = g_{a_1 NN}\overline{\psi}_N\gamma^\mu\gamma^5\vec{\tau}\psi_N\vec{a_1}_\mu \tag{2.90}$$
$$\mathcal{L}_{\pi\pi\rho} = -g_{\pi\pi\rho}[(\partial^\mu\vec{\pi})\times\vec{\pi}]\vec{\rho}_\mu \tag{2.91}$$
$$\mathcal{L}_{\pi\pi\gamma} = -eA_\mu J^\mu_\pi \tag{2.92}$$
$$\mathcal{L}_{\rho\pi\gamma} = e\frac{g_{\pi\rho\gamma}}{4m_\pi}\varepsilon_{\mu\nu\alpha\beta}\mathcal{F}^{\mu\nu}\overline{\rho}^{\alpha\beta}\cdot\vec{\pi} \tag{2.93}$$
$$\mathcal{L}_{a_1\pi\gamma} = -ie\frac{g_{a_1\pi\gamma}}{m_\pi}\vec{a_1}_\mu\mathcal{F}^{\mu\nu}\cdot\partial_\nu\vec{\pi} \tag{2.94}$$
$$\tag{2.95}$$

The coupling constants can be computed from the corresponding decay widths. This will be done in Section 3.2.

3 Calculations

3.1 Kinematics

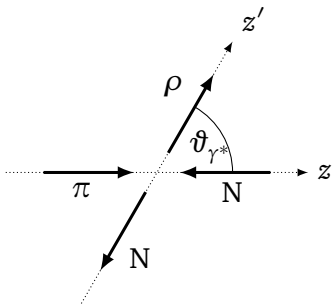

Figure 3.1.: Kinematics of the $\pi N \to \rho N$ reaction in the CM frame

We use the same kinematics as seen in Figure 2.3 which we show again in Figure 3.1 for convenience. The direction of incoming momentum was chosen along the z-axis. We use p for the four-momenta and q for the modulus of the three-momenta.

$$p_\pi = \begin{pmatrix} \sqrt{m_\pi^2 + q_{\text{in}}^2} \\ 0 \\ 0 \\ q_{\text{in}} \end{pmatrix}, \qquad p_N = \begin{pmatrix} \sqrt{m_N^2 + q_{\text{in}}^2} \\ 0 \\ 0 \\ -q_{\text{in}} \end{pmatrix}. \tag{3.1}$$

The calculation of the incoming momentum is straightforward. We use that $s = (p_\pi + p_N)^2$. Thus the CM-energy is simply given by $\sqrt{s}$. Now

$$q_{\text{in}} = \frac{\sqrt{\lambda(s, m_\pi^2, m_N^2)}}{2\sqrt{s}}, \tag{3.2}$$

where $\lambda(x,y,z) = x^2 + y^2 + z^2 - 2(xy + yz + zx)$ is the Källén function.
We choose the production plane to be at $\varphi = 0$, which results in the following outgoing momenta

$$p_\rho = \begin{pmatrix} \sqrt{m_{\text{inv}}^2 + q_{\text{out}}^2} \\ 0 \\ q_{\text{out}} \sin\vartheta_{\gamma^*} \\ q_{\text{out}} \cos\vartheta_{\gamma^*} \end{pmatrix}, \qquad p_{\overline{N}} = \begin{pmatrix} \sqrt{m_N^2 + q_{\text{out}}^2} \\ 0 \\ -q_{\text{out}} \sin\vartheta_{\gamma^*} \\ -q_{\text{out}} \cos\vartheta_{\gamma^*} \end{pmatrix}. \tag{3.3}$$

Here, m_{inv} denotes the invariant mass of the lepton pair and $\overline{N}$ the outgoing nucleon. Likewise

$$q_{\text{out}} = \frac{\sqrt{\lambda(s, m_{\text{inv}}^2, m_N^2)}}{2\sqrt{s}}. \tag{3.4}$$

The polarisation tensor of the photon has been regarded in its rest frame. It decays into the lepton pair, whose momenta have to be transformed from its very CM-system to the CM-system of the incoming pion

and nucleon. We first boost along the z' axis with momentum q_{out}, and then inversely rotate around the scattering angle ϑ_{γ^*}. A boost along the z-axis can be represented by the matrix

$$\mathcal{B}_{\mu\nu}(q,m) = \begin{pmatrix} \gamma(q,m) & 0 & 0 & \gamma(q,m)\beta(q,m) \\ 0 & 1 & 0 & 0 \\ 0 & 0 & 1 & 0 \\ \gamma(q,m)\beta(q,m) & 0 & 0 & \gamma(q,m) \end{pmatrix}_{\mu\nu}, \tag{3.5}$$

with $\gamma(q,m) = \frac{\sqrt{q^2+m^2}}{m}$ and $\beta(q,m) = \frac{q}{m}$. To align the z'-axis with the z-axis, we have to rotate around the y-axis. Such a rotation is represented by

$$\mathcal{R}^{\mu\nu}(\alpha) = \begin{pmatrix} 1 & 0 & 0 & 0 \\ 0 & \cos\alpha & 0 & \sin\alpha \\ 0 & 0 & 1 & 0 \\ 0 & -\sin\alpha & 0 & \cos\alpha \end{pmatrix}^{\mu\nu}. \tag{3.6}$$

Thus, we find the transformation for the polarisation vectors from the photon rest frame to the πN CM frame to be

$$\epsilon'_{\mu}(\lambda) = \mathcal{R}^{\mu\nu}(-\vartheta_{\gamma^*})\mathcal{B}_{\nu\xi}(q_{\text{out}}, m_{\text{inv}})\epsilon^{\xi}(\lambda). \tag{3.7}$$

3.2 Coupling Constants

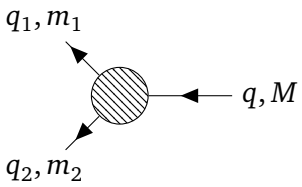

Figure 3.2.: Two particle decay kinematics as used in [19]

The total decay width for a two particle decay is given by

$$\Gamma = \frac{1}{32\pi^2}\frac{q_1}{M^2}\int \mathrm{d}\Omega\,|\mathcal{M}|^2, \tag{3.8}$$

where $q = \frac{\sqrt{\lambda(M^2,m_1^2,m_2^2)}}{2M}$ and $\mathrm{d}\Omega = \mathrm{d}\varphi_1 \mathrm{d}\cos\vartheta_1$. The kinematics are shown in Figure 3.2. This allows us to fix the various coupling constants from the interaction Lagrangians. The necessary data is shown in Table 3.1 and was accumulated from "Review of Particle Physics" (2018) [19]. The value for the decay width was calculated from the total decay width value times the average of the lower and upper value for the branching ratio of the respective decay channel. For the decay ratio of a nucleon resonance into a ρ-meson, we followed the assumptions of [2] and taken his values as were the values for the 3/2 resonances. The branching ratios N $\to \gamma$p and N $\to \gamma$n have been added together and treated as the decay N $\to \gamma$N. The value of the a_1 resonance width was taken from "Review of Particle Physics" (2014, updated 2015) [20].

particle X	J^P	mass	$\Gamma(X \to \pi\pi)$	$g_{X\pi\pi}$	$\Gamma(X \to \rho\pi)$	$g_{X\rho\pi}$	$\Gamma(X \to \gamma\pi)$	$g_{X\gamma\pi}$
N	$1/2^-$	938.27	-	-	-	-	-	-
π	0^-	138.04	-	-	-	-	-	-
ρ	1^-	775.26	149.1	5.998	-	-	0.067	0.058
a_1	1^+	1230	n/a	-	-	-	0.64	0.083
particle X	J^P	mass	$\Gamma(X \to \pi\mathrm{N})$	$g_{X\pi\mathrm{N}}$	$\Gamma(X \to \rho\mathrm{N})$	$g_{X\pi\mathrm{N}}$	$\Gamma(X \to \gamma\mathrm{N})$	$g_{X\gamma\mathrm{p}}$
N(1440)	$1/2^+$	1440	227.5	0.329	40	-	0.0578	-
N(1520)	$3/2^-$	1515	66	0.148	22	17.166	0.242	-
N(1535)	$1/2^-$	1530	63	0.134	3	1.480	0.293	-
Δ(1600)	$3/2^+$	1570	40	0.045	31.25	44.4	0.045	-

Table 3.1.: Masses and decay widths for numerous particles in units of MeV. The coupling constants are dimensionless.

3.3 Invariant Amplitudes

To write down the invariant matrix element we start from the outgoing fermion line and trace it back to the incoming one. We acquire a factor for each vertex $\mathcal{V}$, internal lines represent the propagators, denoted by $\mathcal{P}$. From Fig. 2.6 we see, that the amplitudes are given by

$$\begin{aligned}
\mathcal{M}_{\mathrm{S}}^{\mathrm{prod}}(\lambda) &= \bar{\mathrm{u}}_f \epsilon_\mu^*(\lambda) \left(\mathcal{V}_{\mathrm{RN}\gamma}\mathcal{P}_{\mathrm{R}}\mathcal{V}_{\mathrm{N}\pi\mathrm{R}}\right)^\mu \mathrm{u}_i \\
\mathcal{M}_{\mathrm{T}}^{\mathrm{prod}}(\lambda) &= \bar{\mathrm{u}}_f \left(\mathcal{V}_{\mathrm{N}M\mathrm{N}}\mathcal{P}_M\mathcal{V}_{M\pi\gamma}\right)^\mu \epsilon_\mu^*(\lambda)\mathrm{u}_i \\
\mathcal{M}_{\mathrm{U}}^{\mathrm{prod}}(\lambda) &= \bar{\mathrm{u}}_f \left(\mathcal{V}_{\mathrm{N}\pi\mathrm{R}}\mathcal{P}_{\mathrm{R}}\mathcal{V}_{\mathrm{RN}\gamma}\right)^\mu \epsilon_\mu^*(\lambda)\mathrm{u}_i,
\end{aligned} \tag{3.9}$$

where f and i denote the final and initial fermion respectively and $M \in \{\pi, \rho, a_1\}$. Implementing the VMD model, we aquire an extra factor $F_{\mathrm{VMD}}(p^2)$ for the $\rho\gamma$ vertex and the dressed ρ propagator from Equation (2.62) and Equation (2.75)

$$F_{\mathrm{VMD}}(p^2) = -\frac{ep^2}{g_{\rho\gamma}(p^2) - m_\rho^2 + \mathrm{i}\sqrt{p^2}\Gamma_\rho}. \tag{3.10}$$

Comparing the Lagrangians for the interactions with a ρ and a γ we find a very similar structure, which makes sense, since both are $J^P = 1^-$ particles. Of course, the $\rho^{\mu\nu}$ has been substituted by $\mathcal{F}^{\mu\nu}$. Furthermore, since the electromagnetic force violates isospin (only I, not I_z), there is no isospin structure in its Lagrangian. So a proton can not become a neutron or vice versa by emitting a photon, since $\overline{\psi}_{\mathrm{p}}\psi_{\mathrm{n}} = \overline{\psi}_{\mathrm{n}}\psi_{\mathrm{p}} = 0$. Since both $\mathcal{F}^{\mu\nu}$ and $\rho^{\mu\nu}$ only contribute with their four-momentum, which for momentum conservation reasons is equal, and only the neutral ρ-meson can couple to a photon (with no other particles involved) we can use the direct photon coupling Lagrangian and multiply it with factor $(1 + \overline{\tau}^3 F_{\mathrm{VMD}}(p^2))$ to account for both diagrams.

We see, that each matrix element has the same structure

$$\mathcal{M}_{\mathrm{X}}(\lambda) = \bar{\mathrm{u}}_f \Xi_{\mathrm{X}}^\mu \epsilon_\mu^*(\lambda)\mathrm{u}_i. \tag{3.11}$$

Thus, to calculate the effects of interferences between the different channels, we can simply add the different Ξ^μ together, i.e.

$$\mathcal{M}_{\mathrm{stu}} = \bar{\mathrm{u}}_f \left(\Xi_{\mathrm{s}}^\mu + \Xi_{\mathrm{t}}^\mu + \Xi_{\mathrm{u}}^\mu\right) \epsilon_\mu^*(\lambda)\mathrm{u}_i. \tag{3.12}$$

To calculate the squared matrix element, we use Casimir's Trick Eq. (2.10)

$$\sum |\mathcal{M}|^2 = \sum \mathcal{M}\mathcal{M}^\dagger = \mathcal{T}r\left\{\Xi(\not{p}_i + m)\overline{\Xi}(\not{p}_f + m)\right\}. \tag{3.13}$$

3.4 Numerics

By summing and averaging over the particle spins, we have established in Equation (2.10) that we have to calculate a trace of a matrix product. Usually, one can solve the Dirac traces by using the Dirac algebra from which follows that

$$\mathcal{T}r\{\gamma^\mu\gamma^\nu\} = 4\eta^{\mu\nu}. \tag{3.14}$$

First we want to remind the reader of some trace properties. For the following part, let us consider four quadratic matrices A, B, C and D:

$$\begin{aligned} \mathcal{T}r\{A+B\} &= \mathcal{T}r\{A\} + \mathcal{T}r\{B\} \\ \mathcal{T}r\{\alpha A\} &= \alpha\mathcal{T}r\{A\} \qquad\qquad \alpha\in\mathbb{C} \\ \mathcal{T}r\{ABC\} &= \mathcal{T}r\{BCA\} \\ &= \mathcal{T}r\{CAB\} \end{aligned} \tag{3.15}$$

Applying the anticommutator (Equation (2.5)) we can calculate the trace of two gamma matrices, using that the trace is invariant under cyclic permutation:

$$\mathcal{T}r\{\gamma^\mu\gamma^\nu\} = \mathcal{T}r\{\gamma^\nu\gamma^\mu\} = \mathcal{T}r\left\{\frac{1}{2}\{\gamma^\mu,\gamma^\nu\}\right\} = \mathcal{T}r\{\mathbb{1}\}\,\eta^{\mu\nu} = 4\eta^{\mu\nu}. \tag{3.16}$$

For four gamma matrices, by using the anticommutator relations

$$\{A,BC\} = \{A,B\}C - B[A,C] \tag{3.17}$$

$$\{A,BCD\} = \{A,BC\}D - BC\{A,D\} + B\{A,CD\}, \tag{3.18}$$

we find:

$$\begin{aligned} \mathcal{T}r\{\gamma^\kappa\gamma^\lambda\gamma^\mu\gamma^\nu\} &= \mathcal{T}r\left\{\frac{1}{2}\{\gamma^\kappa,\gamma^\lambda\gamma^\mu\gamma^\nu\}\right\} \\ &= \frac{1}{2}\mathcal{T}r\left\{\{\gamma^\kappa,\gamma^\lambda\gamma^\mu\}\gamma^\nu - \gamma^\lambda\gamma^\mu\{\gamma^\kappa,\gamma^\nu\} + \gamma^\lambda\{\gamma^\kappa,\gamma^\mu\gamma^\nu\}\right\} \\ &= \frac{1}{2}\mathcal{T}r\left\{\{\gamma^\kappa,\gamma^\lambda\}\gamma^\mu\gamma^\nu - \gamma^\lambda\gamma^\mu\{\gamma^\kappa,\gamma^\nu\} + \gamma^\lambda\{\gamma^\kappa,\gamma^\mu\}\gamma^\nu\right\} \\ &= \mathcal{T}r\left\{\eta^{\kappa\lambda}\gamma^\mu\gamma^\nu - \eta^{\kappa\nu}\gamma^\lambda\gamma^\mu + \eta^{\kappa\mu}\gamma^\lambda\gamma^\nu\right\} \\ &= 4\left(\eta^{\kappa\lambda}\eta^{\mu\lambda} - \eta^{\kappa\nu}\eta^{\lambda\mu} + \eta^{\kappa\mu}\eta^{\lambda\nu}\right). \end{aligned} \tag{3.19}$$

The commutator terms that would arise from Equation (3.17) have been neglected since their trace vanishes. Note that we are able to express a trace of four gamma matrices in terms of traces of two gamma matrices. From here we can conclude the recursive formula for the trace of an even number of gamma matrices [21]:

$$\mathcal{T}r\{\gamma^{\nu_1}\dots\gamma^{\nu_n}\} = \sum_{k=2}^{n}(-1)^k\eta^{\nu_1\nu_k}\mathcal{T}r\left\{\gamma^{\nu_2}\dots\cancel{\gamma^{\nu_k}}\dots\gamma^{\nu_n}\right\}. \tag{3.20}$$

The trace of an odd number of gamma matrices vanishes, as follows with the γ^5 anticommutator relation (Equation (2.6)) and the trace properties (Equation (3.15)):

$$\begin{aligned} \mathcal{T}r\left\{\gamma^\lambda\gamma^\mu\gamma^\nu\right\} &= \mathcal{T}r\left\{\gamma^\lambda\gamma^\mu\gamma^\nu\gamma^5\gamma^5\right\} \\ &= \mathcal{T}r\left\{-\gamma^5\gamma^\lambda\gamma^\mu\gamma^\nu\gamma^5\right\} \\ &= -\mathcal{T}r\left\{\gamma^\lambda\gamma^\mu\gamma^\nu\right\} \end{aligned} \tag{3.21}$$

Note that the trace length increases with $(n-1)!! = (n-1)(n-3)\dots 1$, where n is the number of gamma matrices, due to the recursion formula. Therefore a trace of for example 16 gamma matrices, as later found in the amplitudes, yields 2 027 025 terms. Obviously this can not be done by hand in reasonable time. The Mathematica package *FeynCalc* can solve these traces using this Dirac Algebra. However for complicated traces, this takes quite a long time. Therefore we calculate these traces by choosing a representation for the gamma matrices and summing over the indices explicitly. A further speed bonus can be obtained by forcing Mathematica to compute with floating point numbers only (i.e. adding a decimal point to every numerical value). An example can be found in Appendix B.

For later calculations (Section 3.4) we choose the Dirac representation [10]

$$\gamma^0 = \begin{pmatrix} \mathbb{1} & \mathbb{0} \\ \mathbb{0} & -\mathbb{1} \end{pmatrix} \qquad \gamma^k = \begin{pmatrix} \mathbb{0} & \sigma^k \\ -\sigma^k & \mathbb{0} \end{pmatrix}. \tag{3.22}$$

Here, σ^k are the Pauli matrices, where we use the representation of Equation (2.50).

4 Results

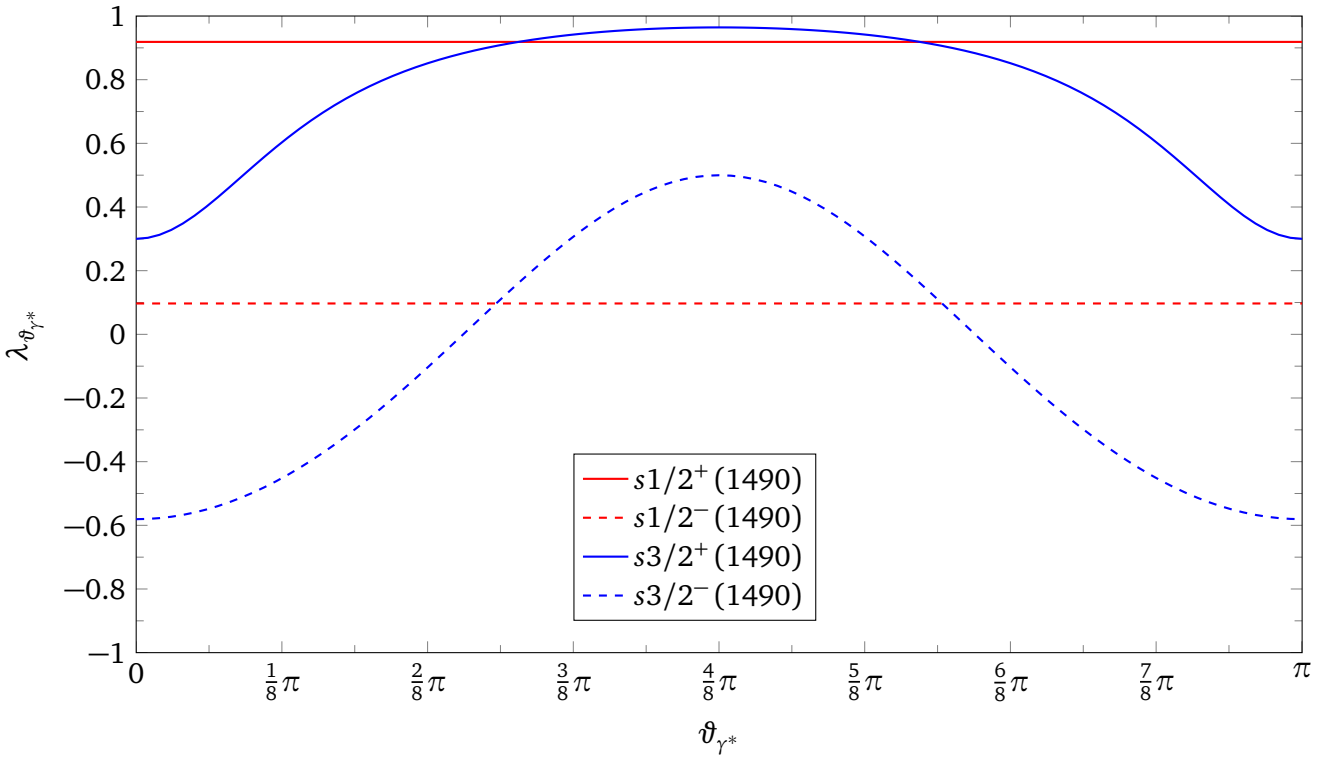

Figure 4.1.: The anisotropy coefficient for hypothetical on-shell resonances for the s-channel, for $\sqrt{s} = 1.49\,\text{GeV}$.

We calculate the anisotropy coefficients Equation (2.39) of the transition $\text{N}\pi \to \text{Ne}^+\text{e}^-$ using the model described above. We set the CM energy to $\sqrt{s} = 1.49\,\text{GeV}$ in accordance with the HADES experiment. As validation and for later comparisons of the impact of the t-channel, we first reproduce the data of [2] in Figure 4.1. Therefore we also assume a hypothetical resonance mass that coincides with the CM energy, i.e. is on-shell. For the regarded transition, we can expand the incoming particles in their eigenstates of orbital angular momentum, following [2]:

$$|\pi(\vec{q}); \text{N}(-\vec{q})\rangle \propto \sum_{l,m} Y^*_{lm}(\vartheta, \varphi)\,|lm\rangle\,, \tag{4.1}$$

where the kinematic parameters were discussed in Section 3.1 and Y^*_{lm} are the spherical harmonic functions. But $Y^*_{lm}(\vartheta = 0, \varphi) \neq 0$ only for $m = 0$, so the z-component of the orbital angular momentum vanishes in the initial state. This means, that the total angular momentum of the resonance state only depends on the spin of the incoming nucleon. Thus, only the resonance's $J_z = \pm 1$ states are populated. This implies, that for an unpolarised nucleon the $J = 1/2$ resonance is also unpolarised, so we expect the anisotropy coefficient in the CM-frame to be independent of ϑ_{γ^*}. Higher spin particles have a non trivial polarisation, which can be non-zero even though the initial states have no preferred direction. This implies an angular anisotropy in the CM mass [2]. Indeed we are able to reproduce the results of Speranza [2] in Figure 4.1. The red lines describe the spin-1/2 and the blue lines the spin 3/2 resonance. Solid lines indicate positive parity while dashed lines mean negative parity. The lines are labelled

with the regarded channel(s), the rest mass of the intermediate particle and finally the parity sign. We find that in the spin-$1/2^{\pm}$ case the anisotropy coefficient is independent of the scattering angle. For the spin-$3/2^{\pm}$ resonances, we find the anisotropy coefficient to be symmetric around $\pi/2$, where it also has a maximum. In both cases, the resonance with positive parity leads to a higher coefficient.

Speranza [2] has concluded that the N(1440) and N(1535) dominate the process in the combined s- and u-channel diagrams for this centre of mass energy. We can now calculate the anisotropy coefficient for various dilepton masses. However, we do not know the relative phase between the two diagrams. For a relative minus sign between the two resonances, we reproduce the result from [2] in Figure 4.2. We see that with decreasing lepton mass the anisotropy coefficient progresses towards $\lambda_\vartheta = 1$. The interpretation is, that for $m \to 0$ the photon becomes real and thus is only allowed to have transversal polarisations.

We now study the effect of the t-channel. As in the work of Speranza, the phase between the diagrams is unknown, therefore we include all intermediate mesons with varying signs for the limit cases where the phase difference is either 0 or π. Figure 4.3 shows the anisotropy coefficient, for the combined interference between the N(1440) and N(1535) in the s- and u-channel and π, ρ and a_1 in the t-channel. For comparison, the anisotropy coefficient from Figure 4.2 for a dilepton mass $m_{\text{inv}} = 500\,\text{MeV}$ is also shown (black dotted line). We find, that the impact of the ρ is negligible, that is, the coefficient does not differ visibly in varying the sign of the corresponding coupling constant. The other two t-channel mesons lead to a splitting up in four curves (two for each meson and sign, as we again do not know the phase difference), which generally share the same shape of the initial curve. Each curve has two intersection points with the reference curve, meaning that the effect of the t-channel interference cancels at this point. We note, that the difference between the individual curves is highest for $\vartheta_{\gamma^*} = \pi$, i.e. transversally emitted photons. The highest deviation from the reference curve is obtained by choosing a relative sign for the coupling constants. A negative sign for the intermediate π-diagram in the t-channel leads to a deviation to higher values for lower ($\vartheta_{\gamma^*} \lesssim \pi/4$) and higher ($\vartheta_{\gamma^*} \gtrsim 19/32\pi$) values of the scattering angle. In

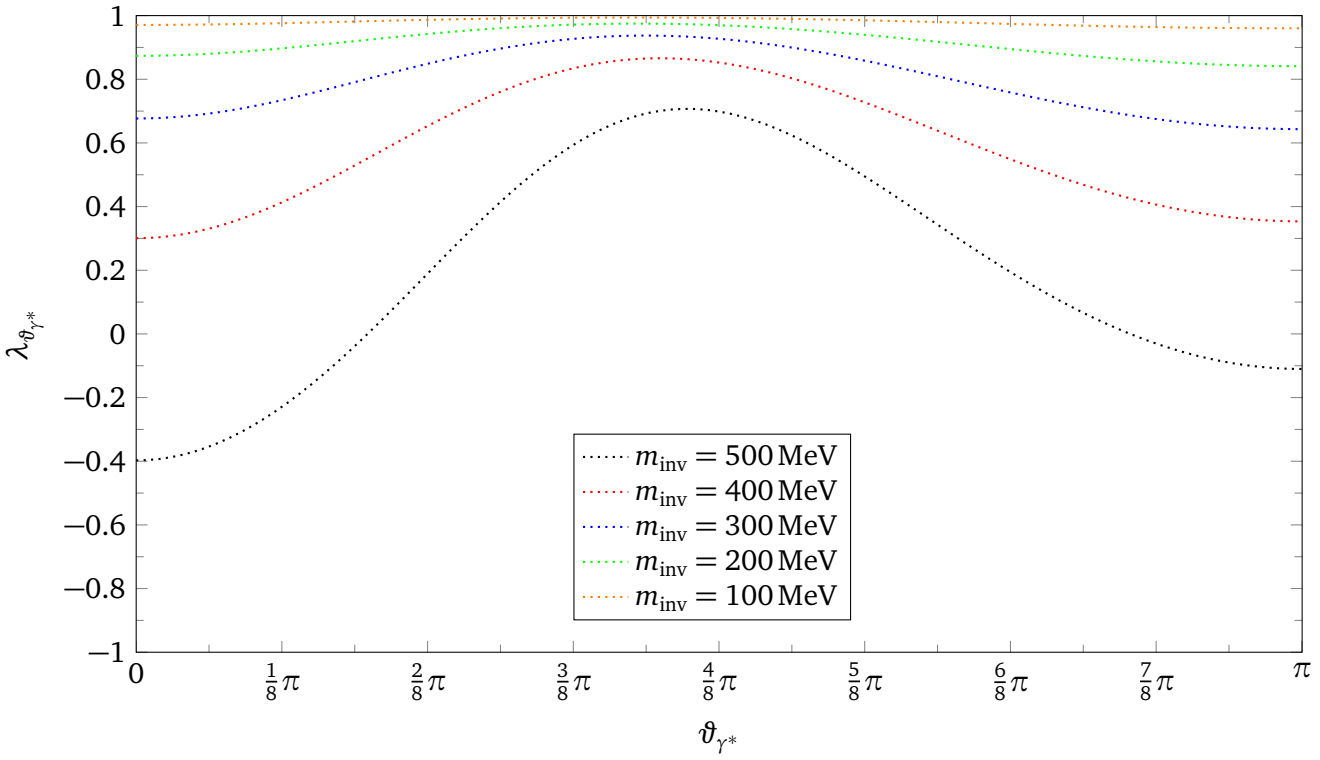

Figure 4.2.: The anisotropy coefficient for the combined N(1440) and N(1535) resonances with s- and u-channel diagrams for various invariant dilepton masses, with $\sqrt{s} = 1.49\,\text{GeV}$.

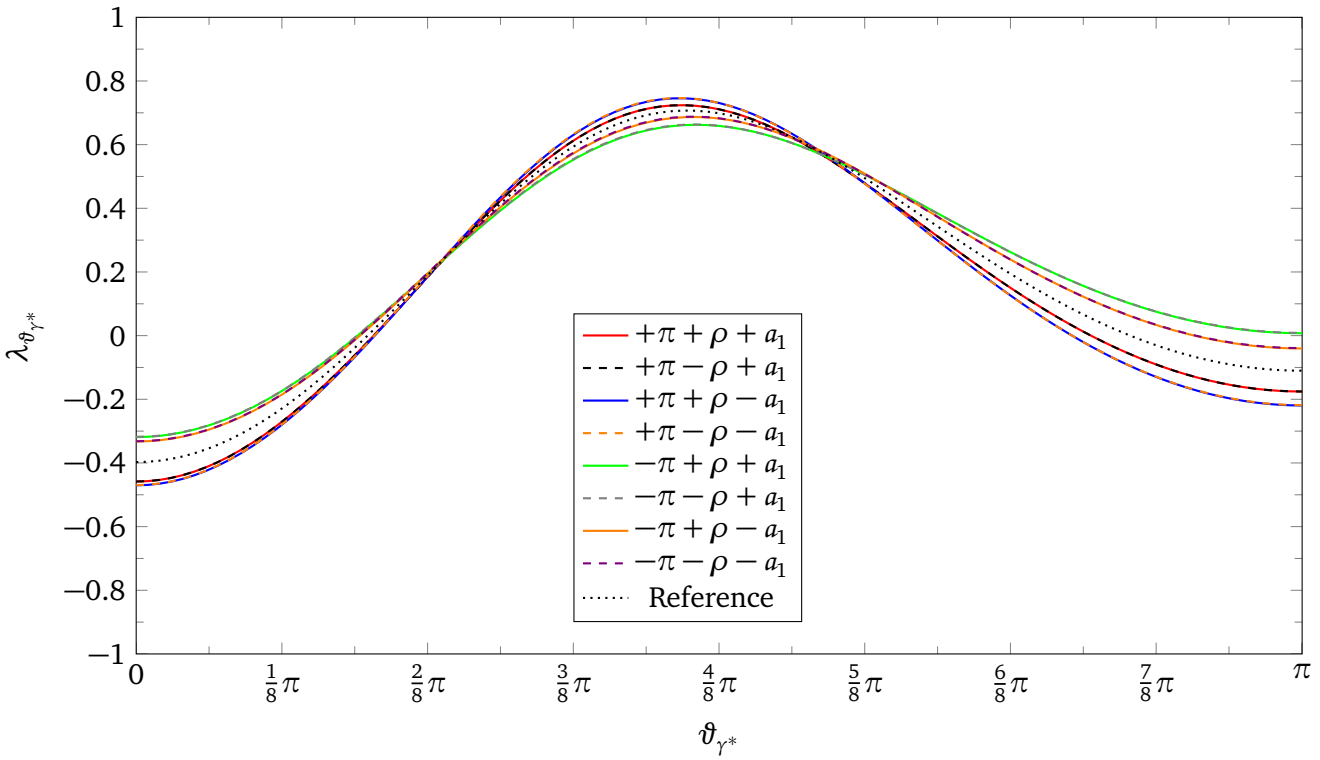

Figure 4.3.: Comparison between the signs for the different intermediate particles in the t-channel for $m_{\text{inv}} = 500\,\text{MeV}$. The reference is the black dotted curve from Figure 4.2 for $m_{\text{inv}} = 500\,\text{MeV}$, without t-channel interference. $\sqrt{s} = 1.49\,\text{GeV}$.

between it has a slightly lower value. For a positive sign of the intermediate π-diagram the roles of lower and upper values are reversed. The a_1 resonance leads to an even smaller deviation, that is best observable for high scattering angles. A negative sign for the a_1-diagram leads to a small offset to lower values in the outer bounds, and shifts the anisotropy coefficient slightly up in between the intersection points.

We now consider varying dilepton masses. We exclude the ρ-meson from the plots to improve clarity as it again has no visible impact. Now the red lines refer to a positive sign for the π-diagrams and the blue lines for a negative one. Solid lines indicate a positive sign for the a_1, dashed ones a negative sign. We find, that for decreasing invariant dilepton mass, the anisotropy coefficient follows the initial shape of the N(1440) and N(1535) interference. This suggests that the s- und u-channel interference dominate the process, while the t-channel only leads to minor variation. Furthermore the intersection points with the reference curve shift to the left with decreasing invariant lepton mass. The impact of the a_1-resonance also decreases with decreasing invariant dilepton mass, as we can see clearest in Figure 4.6 and Figure 4.7, where the difference between the solid and dashed curves is nearly indistinguishable. The biggest deviation for low invariant dilepton masses ($m_{\text{inv}} = 100\,\text{MeV}$) comes for pions with a positive phase. Following the assumption, that $\lambda_\vartheta \to 1$ for $m_{\text{inv}} \to 0$ i.e. as the virtual photons approaches zero rest mass, its longitudinal polarisation must vanish, we can conclude that the positive phase of the π-diagram seems to produce unphysical results.

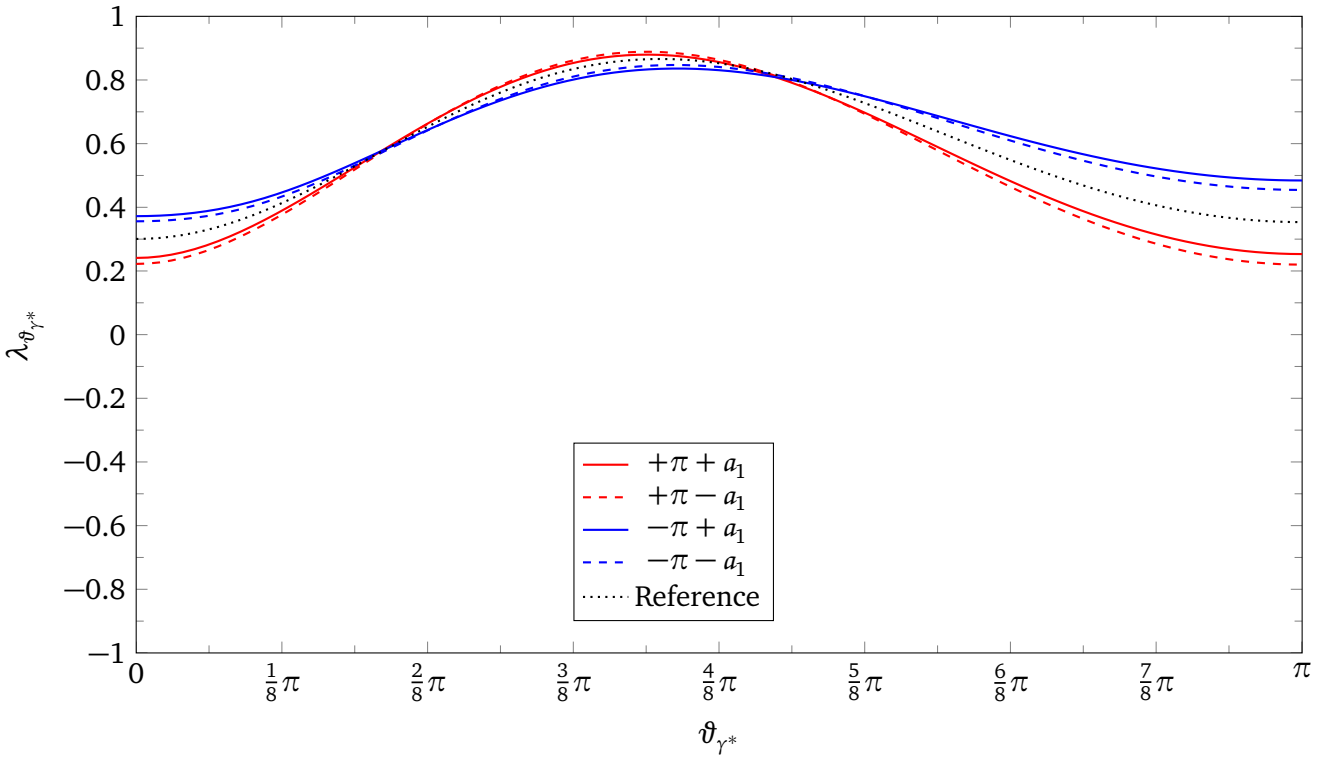

Figure 4.4.: Comparison between the signs for the different intermediate particles in the t-channel for $m_{\text{inv}} = 400\,\text{MeV}$. The reference is the black dotted curve from Figure 4.2 for $m_{\text{inv}} = 400\,\text{MeV}$, without t-channel interference. $\sqrt{s} = 1.49\,\text{GeV}$.

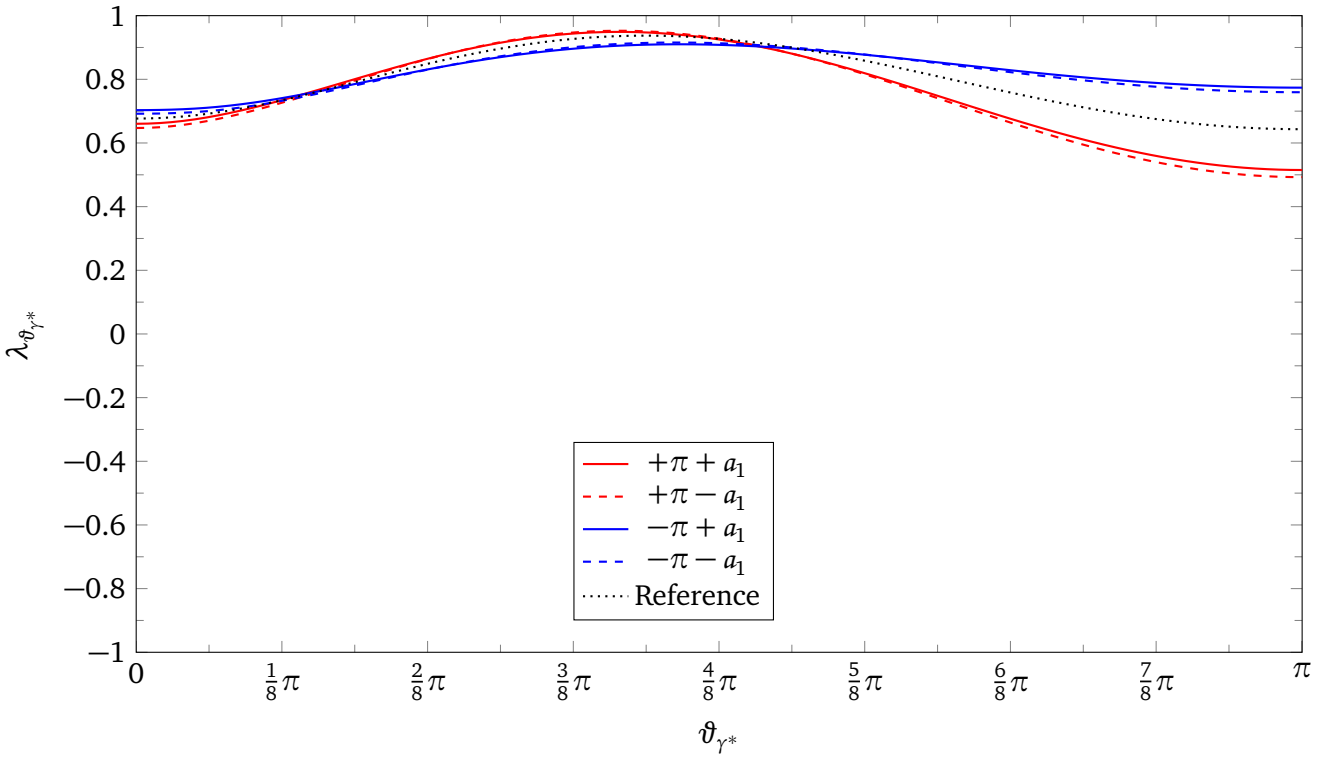

Figure 4.5.: Comparison between the signs for the different intermediate particles in the t-channel for $m_{\text{inv}} = 300\,\text{MeV}$. The reference is the black dotted curve from Figure 4.2 for $m_{\text{inv}} = 300\,\text{MeV}$, without t-channel interference. $\sqrt{s} = 1.49\,\text{GeV}$.

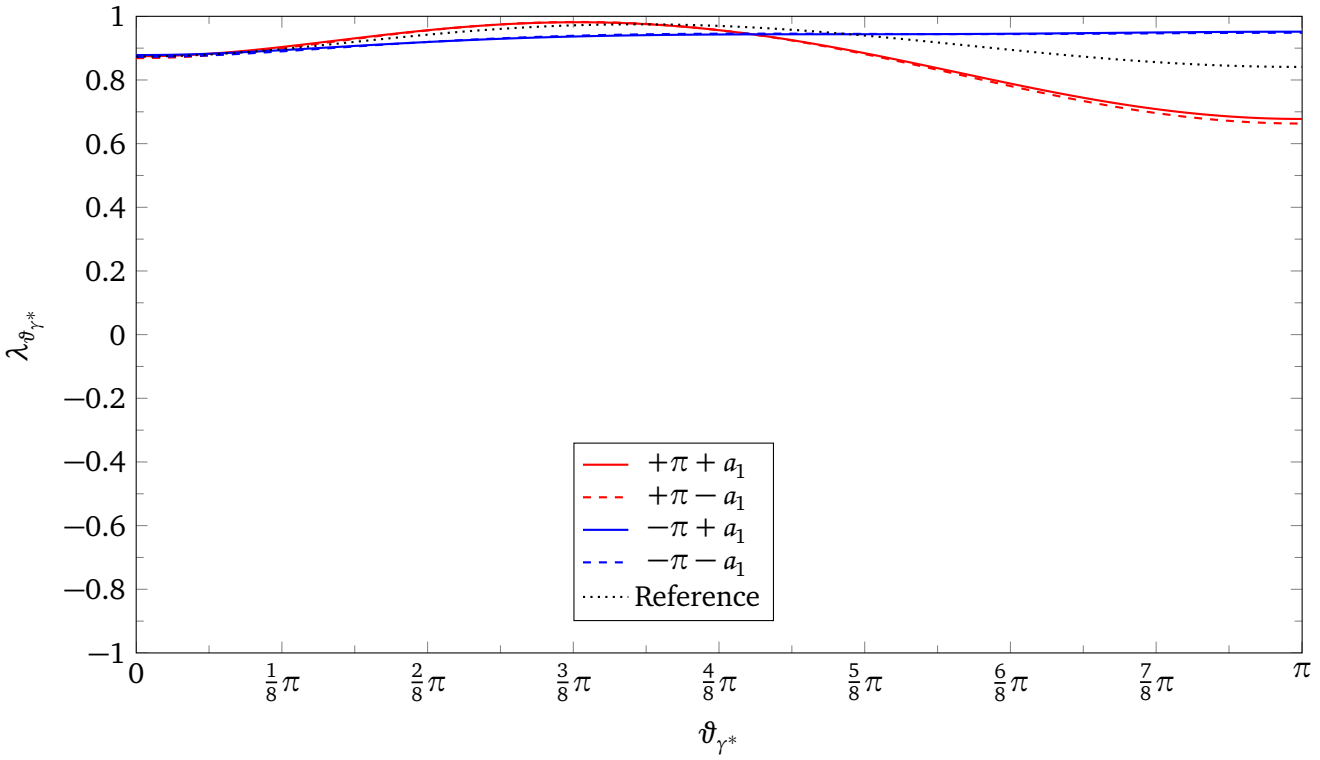

Figure 4.6.: Comparison between the signs for the different intermediate particles in the t-channel for $m_{\text{inv}} = 200\,\text{MeV}$. The reference is the black dotted curve from Figure 4.2 for $m_{\text{inv}} = 200\,\text{MeV}$, without t-channel interference. $\sqrt{s} = 1.49\,\text{GeV}$.

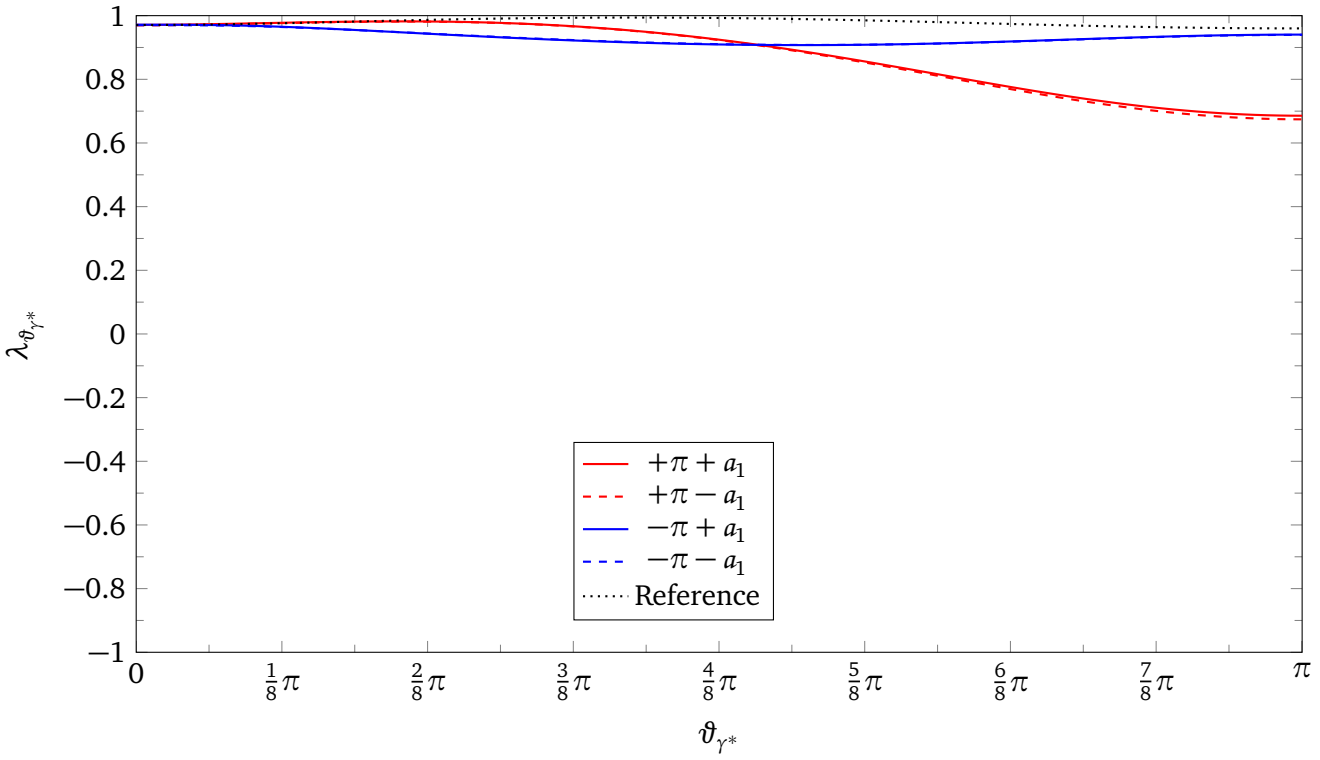

Figure 4.7.: Comparison between the signs for the different intermediate particles in the t-channel for $m_{\text{inv}} = 100\,\text{MeV}$. The reference is the black dotted curve from Figure 4.2 for $m_{\text{inv}} = 100\,\text{MeV}$, without t-channel interference. $\sqrt{s} = 1.49\,\text{GeV}$.

5 Summary and Outlook

In this thesis we have investigated the dilepton anisotropy of the process $\pi N \to Ne^-e^+$. Therefore we have introduced the anisotropy coefficients which depend on the components of the hadron tensor.We have only considered λ_θ, because the total cross section $\sigma \propto 1+\lambda_\vartheta \cos\vartheta$. We developed a powerful and fast script in Mathematica in order to calculate the invariant matrix elements needed for the anisotropy coefficient and extended the existing results of Speranza [2] who discussed the anisotropy coefficient for resonant s- and u-channels. We now implemented the t-channel for intermediate π, ρ-mesons and a_1. We found that the impact of the ρ is negligible. Overall, the process is still dominated by the s- and u-channel diagrams. The contribution of the t-channel leads to a minor shift in the shape of the original s- and u-channel interference. The t-channel is rather dominated by the π while the a_1 leads to more subtle changes. The phase between the diagrams can take a value between 0 and π. We have considered the two extreme cases, leading to a plus or minus sign between the diagrams. Since a real photon can only be transversally polarised, we assume that $\lambda_\vartheta \to 1$ for $m_{\text{inv}} \to 0$. Following this assumption, we conclude that choosing no phase (leading to a positive sign) for the intermediate π-diagram in the t-channel yields unphysical results.

Interesting points left to investigate are the dependencies on the CM-energy, which would like cause a shift in the dominant resonances and the effects of the t-channel on the cross section, which we could not investigate due to time constraints. It would also be compelling to test the model dependency of this effective Lagrangian approach with a different set of Lagrangians. Another point for future research would be the consideration of the ω-meson which also contributes to the VMD in the dilepton creation process. Finally, Speranza also considered dilepton production and anisotropy in heavy ion collision in the s- and u-channel. One could also implement the t-channel in those computations to give a fuller picture.

6 Acknowledgements

First and foremost I'd like to thank my supervisor Michael Buballa who suggested this highly interesting topic, always had an open ear for me and patiently answered my questions. In the many discussions we had, I learned a lot about how to tackle problems in physics and deepened my knowledge of quantum field theory.
I also wish to thank Bengt Friman and Tetyana Galatyuk for insightful discussions and suggesting the possibility to continue working in this field. Furthermore a big *grazie* to Enrico Speranza who was very eager to help and explain his work to me. It was a great opportunity to be able to work with him and he was able to lift my mood many times. I want to thank Martin, Vincent, Thomas, Max, Niels and Daniel for the fun times and advice they offered. I could not have wished for better colleagues.
I'd like to thank Malte for countless discussions and rubber ducking through my thought processes. Finally I want to express my greatest gratitude to my mother, who supported me morally and financially through my entire studies.

A Feynman Rules

Here we will give the Feynman rules necessary for calculating the matrix elements. We use the method of [9]. To get $-i\mathcal{M}$ we multiply the interaction Lagrangian term by i, transform into momentum space by using $\partial_\mu = -ip_\mu$ and finally removing all the fields. Keep in mind that we may arbitrarily relabel contracted terms (that is $a_\mu b^\mu = a_\xi b^\xi$). For better readability we will temporarily omit constants. We will also rewrite vector and matrix multiplication with explicit indices to allow for easier manipulation.

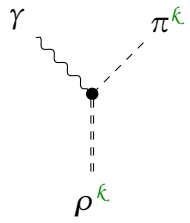

$$\begin{aligned}
\mathscr{L}_{\pi\rho\gamma} &= e\frac{g_{\rho\pi\gamma}}{4m_\pi}\varepsilon_{\mu\nu\alpha\beta}\mathcal{F}^{\mu\nu}\overline{\rho}^{\alpha\beta}\cdot\vec{\pi} \\
(\cdot i) &\propto -i\varepsilon_{\mu\nu\alpha\beta}(\partial^\mu A^\nu - \partial^\nu A^\mu)(\partial^\alpha \rho^{k\beta} - \partial^\beta \rho^{k\alpha})\pi^k \\
(\partial \to ip) &= \varepsilon_{\mu\nu\alpha\beta}(p_\gamma^\mu A^\nu - p_\gamma^\nu A^\mu)(p_\rho^\alpha \rho^{k\beta} - p_\rho^\beta \rho^{k\alpha})\pi^k \\
\text{(remove fields)} &\to \frac{-ieg_{\rho\pi\gamma}}{m_\pi}\varepsilon_{\mu\nu\alpha\beta}p_\gamma^\mu p_\rho^\nu
\end{aligned} \tag{A.1}$$

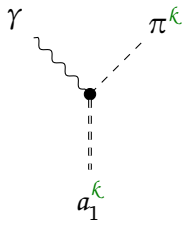

$$\begin{aligned}
\mathscr{L}_{\pi a_1\gamma} &= -ie\frac{g_{a_1\pi\gamma}}{m_\pi}\vec{a}_{1\mu}\mathcal{F}^{\mu\nu}\cdot\partial_\nu\vec{\pi} \\
(\cdot i) &\propto a_1{}^k{}_\mu(\partial^\mu A^\nu - \partial^\nu A^\mu)\partial_\nu\pi^k \\
(\partial \to ip) &= -a_1{}^k{}_\mu(p_\gamma^\mu A^\nu - p_\gamma^\nu A^\mu)p_{\pi\nu}\pi^k \\
\text{(remove fields)} &\to (p_\gamma^\mu p_\pi^\nu - (p_\gamma\cdot p_\pi)\eta^{\mu\nu})
\end{aligned} \tag{A.2}$$

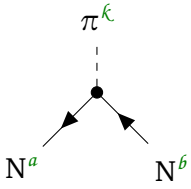

$$\begin{aligned}
\mathscr{L}_{\mathrm{NN}\pi} &= -\frac{f_{\mathrm{NN}\pi}}{m_\pi}\overline{\psi}_{\mathrm{N}}\gamma^5\gamma^\mu\vec{\tau}\psi_{\mathrm{N}}\cdot\partial_\mu\vec{\pi} \\
(\cdot i) &\Rightarrow -i\overline{\psi}^a_{\mathrm{N}}\gamma^5\gamma^\mu\tau^k_{ab}\psi^b_{\mathrm{N}}\partial_\mu\pi^k \\
(\partial \to -ip) &\propto -\overline{\psi}^a_{\mathrm{N}}\gamma^5\gamma^\mu\tau^k_{ab}\psi^b_{\mathrm{N}}p_{\pi\mu}\pi^k \\
\text{(remove fields)} &\propto -\gamma^5\not{p}_\pi\tau^k_{ab} \\
&\Rightarrow \frac{f_{\mathrm{NN}\pi}}{m_\pi}\not{p}_\pi\gamma^5\tau^k_{ab}
\end{aligned} \tag{A.3}$$

The other rules are given by

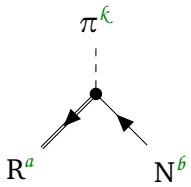

$$-\frac{g_{\mathrm{RN}\pi}}{m_\pi}\Gamma\tau^k{}_{ab}\not{p}_\pi \tag{A.4}$$

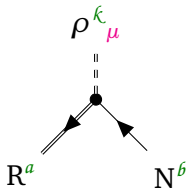

$$\frac{g_{\mathrm{RN}\rho}}{m_\rho}\tilde{\Gamma}\sigma^{\alpha\mu}p_{\rho\alpha}\tau^k{}_{ab} \tag{A.5}$$

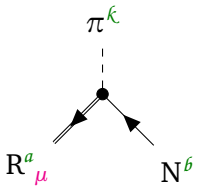

$$-i\frac{g_{RN\pi}}{m_\pi^2}\left(\gamma^\mu(p_R\cdot p_\pi)-p_\pi^\mu \not{p}_R\right)\Gamma\tau^k_{ab} \tag{A.6}$$

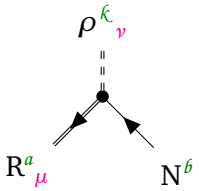

$$i\frac{g_{RN\rho}}{4m_\rho^2}\left(p_\rho^\alpha\gamma^\nu-\eta^{\alpha\nu}\not{p}_\rho\right)\left(p_{R\alpha}\gamma_\mu-\eta_{\alpha\mu}\not{p}_R\right)\tilde{\Gamma}\tau^k_{ab} \tag{A.7}$$

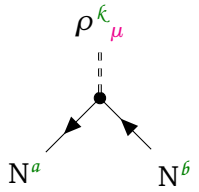

$$\frac{g_{\rho NN}}{2}\left(\gamma^\mu-\frac{\kappa_\rho}{2m_N}\sigma^{\mu\nu}p_{\rho\nu}\right)\tau^k_{ab} \tag{A.8}$$

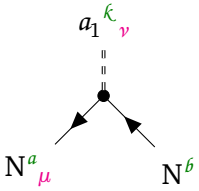

$$g_{a_1NN}\gamma^\mu\gamma^5\tau^k_{ab} \tag{A.9}$$

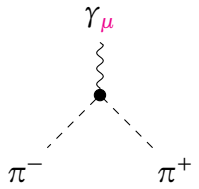

$$e(p_\pi^+-p_\pi^-)^\mu \tag{A.10}$$

B Mathematica Code

Here we provide a sample code for the simple transition in the s-channel. Since we do the summation explicitly, we have to pay attention to the contra- and covariant position of the indices. An appended *C* to the variable name indicates that it is covariant, while no suffix means it is contravariant. We first define the explicit covariant formalism:

In[1]:=
```
GA[0] = ArrayFlatten [{{PauliMatrix[0], 0}, {0, -PauliMatrix[0]}}];
GA[1] = ArrayFlatten[{{0, PauliMatrix[1]}, {-PauliMatrix[1], 0}}];
GA[2] = ArrayFlatten[{{0, PauliMatrix[2]}, {-PauliMatrix[2], 0}}];
GA[3] = ArrayFlatten[{{0, PauliMatrix[3]}, {-PauliMatrix[3], 0}}];
GA[5] = I GA[0].GA[1].GA[2].GA[3];
metricTensor = DiagonalMatrix[{1, -1, -1, -1}];
MT[0, 0] = 1;
MT[1, 1] = MT[2, 2] = MT[3, 3] = -1;
MT[a_, b_] = 0;
GS[a_] := Sum[a[[i + 1]] GA[i] MT[i, i], {i, 0, 3}] // Quiet;
GAC[a_] := MT[a, a] GA[a];
dotP[a_, b_] := a.metricTensor.b;
commutator[a_, b_] := a.b - b.a;
diracSigma[a_, b_] := I/2 commutator[a, b];
matrix[a_] := DiagonalMatrix[{a, a, a, a}];
FV[p_, a_] := p[[a + 1]] // Quiet;
FVC[p_, a_] := (metricTensor.p)[[a + 1]] // Quiet;
diracConjugate[m_] := GA[0].ConjugateTranspose[m].GA[0];
diracDelta[mu_, nu_] := If[mu == nu, 1, 0, 0];
epsTensor[a_, b_, c_, d_] :=
LeviCivitaTensor[4][[a + 1, b + 1, c + 1, d + 1]];
```

We use the same momenta as in Section 3.1 and polarisation vectors from Section 2.2.

In[2]:=
```
pNucleonIn[qIn_] := {Sqrt[massNucleon^2 + qIn^2], 0, 0, -qIn};
pPionIn[qIn_] := {Sqrt[massPion^2 + qIn^2], 0, 0, qIn};
pNucleonOut[qOut_] := {Sqrt[massNucleon^2 + qOut^2], -Sin[tgs] qOut,
        0, -Cos[tgs] qOut}; (* tgs is theta gamma star, the photon \
polarization and scattering angle *)
pResonanceS[mandelstamS_] := {Sqrt[mandelstamS], 0, 0, 0};
epsRF[-1] = 1/Sqrt[2] {0, 1, -I, 0};
epsRF[0] = {0, 0, 0, 1};
epsRF[1] = 1/Sqrt[2] {0, -1, -I, 0};
```

Where the transformation matrix has been defined by

```
In[3]:= lorentzRotate = {{1, 0, 0, 0}, {0, Cos[-tgs], 0, Sin[-tgs]}, {0, 0, 1,
                  0}, {0, -Sin[-tgs], 0, Cos[-tgs]}};
        lorentzGamma[qOut_, massInvariant_] :=
        Sqrt[massInvariant^2 + qOut^2]/massInvariant // Simplify;
        lorentzBeta[qOut_,
        massInvariant_] := -qOut/Sqrt[massInvariant^2 + qOut^2] // Simplify;
        lorentzBoost[qOut_,
        massInvariant_]  := {{lorentzGamma[qOut, massInvariant], 0, 0,
                  lorentzBeta[qOut, massInvariant] *
                  lorentzGamma[qOut, massInvariant]}, {0, 1, 0, 0}, {0, 0, 1,
                  0}, {lorentzBeta[qOut, massInvariant] *
                  lorentzGamma[qOut, massInvariant], 0, 0,
                  lorentzGamma[qOut, massInvariant]}} // Simplify;
        transformRFtoCM[qOut_, massInvariant_] :=
        Inverse[lorentzBoost[qOut, massInvariant].lorentzRotate] //
        Simplify;
```

Finally the actual computation for the anisotropy coefficient Equation (2.39).

```
In[4]:= lambdaTheta[mandelstamS_, invariantMass_, lmbd_, massResonance_] :=
        Module[{s = mandelstamS, invM = invariantMass, lambda,
                mR = massResonance, qIn, qOut, eps, rhoProd},

        qIn = Sqrt[kallenLambda[s, massNucleon^2, massPion^2]]/(2 Sqrt[s]);
        qOut = Sqrt[kallenLambda[s, massNucleon^2, invM^2]]/(2 Sqrt[s]);
        lambda[0] = lmbd[0, s, mR, qIn, qOut, invM];
        lambda[1] = lmbd[1, s, mR, qIn, qOut, invM];
        lambda[2] = lmbd[2, s, mR, qIn, qOut, invM];
        lambda[3] = lmbd[3, s, mR, qIn, qOut, invM];
        eps[1] = Chop[transformRFtoCM[qOut, invM].epsRF[1]];
        eps[-1] = Chop[transformRFtoCM[qOut, invM].epsRF[-1]];
        eps[0] = Chop[transformRFtoCM[qOut, invM].epsRF[0]];
        rhoProd[k_] :=
        Tr[Sum[FVC[Conjugate[eps[k]], mu] FVC[eps[k],
        nu] lambda[
        mu].(GS[{Sqrt[qIn^2 + massNucleon^2], 0, 0, -qIn}] +
        matrix[massNucleon]).diracConjugate[
        lambda[nu]].(GS[{Sqrt[
                qOut^2 + massNucleon^2], -qOut Sin[tgs],
                0, -qOut Cos[tgs]}] + matrix[massNucleon]), {mu, 0,
                3}, {nu, 0, 3}]];
        rhoProdP = rhoProd[1];
        rhoProdM = rhoProd[-1];
        rhoProdZ = rhoProd[0];

        Return[ (rhoProdP + rhoProdM - 2 rhoProdZ)/(rhoProdP + rhoProdM +
        2 rhoProdZ)];
        ];
```

We can now define our vertex factors and propagators. Pay attention to the covariant and contravariant matrices and vectors.

In[5]:=
```
vertexRNPi12p[mR_, qIn_] := -gRNPi[mR]/massPion GA[5].GS[pPionIn[qIn]];
vertexRNRho12p[mu_, mR_, qOut_, massInvariant_] :=
gRNRho[mR]/
massRho diracSigma[GS[pRhoOut[qOut, massInvariant]], GA[mu]];
resonanceDelta[mR_] := (mR - massNucleon - massPion)^2 +
decayWidth[mR]^2/4;
resonanceWidth[p_, mR_, qIn_, l_] :=
decayWidth[mR] mR/
Sqrt[dotP[p, p]] (qIn/(
Sqrt[kallenLambda[mR^2, massNucleon^2,
massPion^2]]/(2 mR)))^(2 l + 1)
propagator12[p_, m_, qIn_] := (GS[p] + matrix[m])/(
dotP[p, p] - m^2 + I Sqrt[dotP[p, p]] resonanceWidth[p, m, qIn, 0])
```

To finally calculate the anisotropy coefficient, simply write down the matrix element.

In[6]:=
```
matrixS12p[mu_, s_, mR_, qIn_, qOut_, massInvariant_] :=
vertexRNRho12p[mu, mR, qOut, massInvariant].propagator12[
pResonanceS[s], mR, qIn].vertexRNPi12p[mR, qIn];
lambdaTheta[mandelstamS, massInvariant, matrixS12p, massResonance];
```

C References

[1] Enrico Speranza, Miklós Zétényi, and Bengt Friman. "Polarization and dilepton anisotropy in pion-nucleon collisions". In: *Phys. Lett.* B764 (2017), pp. 282–288. DOI: 10.1016/j.physletb.2016.11.015. arXiv: 1605.04954 [hep-ph].

[2] Enrico Speranza. "Virtual photon polarization and dilepton anisotropy in pion-nucleon and heavy-ion collisions". PhD thesis. Technische Universität Darmstadt, 2017. URL: http://tuprints.ulb.tu-darmstadt.de/7460.

[3] P. Jain and Y. Kumar. "Photon Emission from Quark Gluon Plasma at RHIC and LHC". In: *Journal of Modern Physics* 5 (2014), pp. 686–692. DOI: {10.4236/jmp.2014.58080.}.

[4] G. Agakishiev et al. "Dielectron production in Ar+KCl collisions at 1.76A GeV". In: *Phys. Rev.* C84 (2011), p. 014902. DOI: 10.1103/PhysRevC.84.014902. arXiv: 1103.0876 [nucl-ex].

[5] W. K. et al. Wilson. "Inclusive dielectron cross sections in $p + p$ and $p + d$ interactions at beam energies from 1.04 to 4.88 GeV". In: *Phys. Rev. C* 57 (4 Apr. 1998), pp. 1865–1878. DOI: 10.1103/PhysRevC.57.1865. URL: https://link.aps.org/doi/10.1103/PhysRevC.57.1865.

[6] E. L. Bratkovskaya, O. V. Teryaev, and V. D. Toneev. "Anisotropy of dilepton emission from nuclear collisions". In: *Phys. Lett.* B348 (1995), pp. 283–289. DOI: 10.1016/0370-2693(95)00164-G.

[7] Michael E. Peskin and Daniel V. Schroeder. *An Introduction to quantum field theory*. Reading, USA: Addison-Wesley, 1995. ISBN: 9780201503975, 0201503972. URL: http://www.slac.stanford.edu/~mpeskin/QFT.html.

[8] Walter Greiner and Joachim Reinhardt. *Field Quantization*. Springer Berlin Heidelberg, 1996.

[9] K. Kumericki. "Feynman Diagrams for Beginners". In: *ArXiv e-prints* (Feb. 2016). Provided by the SAO/NASA Astrophysics Data System. arXiv: 1602.04182 [physics.ed-ph]. URL: http://adsabs.harvard.edu/abs/2016arXiv160204182K.

[10] David J Griffiths. *Introduction to elementary particles; 2nd rev. version*. Physics textbook. New York, NY: Wiley, 2008. URL: https://cds.cern.ch/record/111880.

[11] Michael Urban. "Impulsunabhängigkeit des ρ-Meson-Propagators in kalter Kernmaterie". Diploma thesis. Technische Hochschule Darmstadt, 1997.

[12] J.J Sakurai. "Theory of strong interactions". In: *Annals of Physics* 11.1 (1960), pp. 1–48. ISSN: 0003-4916. DOI: https://doi.org/10.1016/0003-4916(60)90126-3. URL: http://www.sciencedirect.com/science/article/pii/0003491660901263.

[13] J. J. (Jun John) Sakurai. *Currents and mesons*. Based on the version of the author's lectures presented in summer 1967 at the University of Chicago. Chicago : University of Chicago Press, 1969.

[14] Norman M. Kroll, T. D. Lee, and Bruno Zumino. "Neutral Vector Mesons and the Hadronic Electromagnetic Current". In: *Phys. Rev.* 157 (5 May 1967), pp. 1376–1399. DOI: 10.1103/PhysRev.157.1376. URL: https://link.aps.org/doi/10.1103/PhysRev.157.1376.

[15] James D Bjorken and (joint author.) Drell Sidney D. (Sidney David). *Relativistic quantum fields*. New York : McGraw-Hill, 1965. ISBN: 0070054940.

[16] V. Pascalutsa. "Correspondence of consistent and inconsistent spin - 3/2 couplings via the equivalence theorem". In: *Phys. Lett.* B503 (2001), pp. 85–90. DOI: 10.1016/S0370-2693(01)00140-X. arXiv: hep-ph/0008026.

[17] V. Pascalutsa. “Quantization of an interacting spin-$\frac{3}{2}$ field and the Δ isobar”. In: *Phys. Rev. D* 58 (9 Sept. 1998), p. 096002. DOI: 10.1103/PhysRevD.58.096002. URL: https://link.aps.org/doi/10.1103/PhysRevD.58.096002.

[18] M. Zétényi and G. Wolf. “Dilepton production in pion-nucleon collisions in an effective field theory approach”. In: *PhysRevC* 86.6, 065209 (Dec. 2012), p. 065209. DOI: 10.1103/PhysRevC.86.065209. arXiv: 1208.5671 [nucl-th]. URL: http://adsabs.harvard.edu/abs/2012PhRvC..86f5209Z.

[19] M. Tanabashi et al. “Review of Particle Physics”. In: *Phys. Rev. D* 98 (3 Aug. 2018), p. 030001. DOI: 10.1103/PhysRevD.98.030001. URL: https://link.aps.org/doi/10.1103/PhysRevD.98.030001.

[20] K.A. Olive et al. “Review of Particle Physics”. In: *Chin. Phys. C* 38 (2014), p. 090001. URL: http://pdg.lbl.gov/2015/.

[21] Vadim Kaplunovsky. *Dirac Trace Techniques*. 2008. URL: http://bolvan.ph.utexas.edu/~vadim/classes/2008f.homeworks/traceology.pdf.